Radiocarbon Analysis of Elemental and Organic Carbon in Switzerland during Winter-Smog Episodes from 2008 to 2012 – Part I: Source Apportionment and Spatial Variability

P. Zotter[1], V.G. Ciobanu[1,*], Y.L. Zhang[1,2,3,4], I. El-Haddad[1], M. Macchia[5], K. R. Daellenbach[1], G. A. Salazar[2,3], R.-J. Huang[1], L. Wacker[6], C. Hueglin[7], A. Piazzalunga[8], P. Fermo[9], M. Schwikowski[2,3,4], U. Baltensperger[1], S. Szidat[2,3], A.S.H. Prévôt[1]

[1]{Laboratory of Atmospheric Chemistry, Paul Scherrer Institute (PSI), 5232 Villigen PSI, Switzerland}

[2]{Department of Chemistry and Biochemistry, University of Bern, Bern, Switzerland}

[3]{Oeschger Centre for Climate Change Research, University of Bern, Bern, Switzerland}

[4]{Laboratory of Radiochemistry and Environmental Chemistry, Paul Scherrer Institute (PSI), 5232 Villigen PSI, Switzerland}

[5]{CEDAD-Department of Engineering for Innovation, University of Salento, Lecce, Italy}

[6]{Laboratory of Ion Beam Physics, ETH Hönggerberg, Zürich, Switzerland}

[7]{Laboratory for Air Pollution and Environmental Technology, Swiss Federal Laboratories for Materials Science and Technology (Empa), Überlandstrasse 129, 8600 Dübendorf, Switzerland}

[8]{University of Milano Bicocca, Department of Earth and Environmental Sciences, 20126 Milano, Italy}

[9] Department of Chemistry, University of Milano, 20133 Milano, Italy

[*]{now at: Centre for Ice and Climate, Niels Bohr Institute, University of Copenhagen, Copenhagen, Denmark}

Correspondence to: A.S.H. Prévôt (andre.prevot@psi.ch)

Abstract

While several studies have investigated winter-time air pollution with a wide range of concentration levels, hardly any results are available for longer time periods covering several winter-smog episodes at various locations; e.g. often only a few weeks from a single winter are investigated. Here, we present source apportionment results of winter-smog episodes from 16 air pollution monitoring stations across Switzerland from 5 consecutive winters. Radiocarbon (^{14}C) analyses of the elemental (EC) and organic (OC) carbon fractions, as well as levoglucosan, major water-soluble ionic species and gas-phase pollutant measurements were used to characterize the different sources of PM_{10}. The most important contributions to PM_{10} during winter-smog episodes in Switzerland were on average the secondary inorganic constituents (sum of nitrate, sulfate and ammonium = 41 ± 15%) followed by organic matter OM (34 ± 13%) and EC (5 ± 2%). The non-fossil fractions of OC ($f_{NF,OC}$) ranged on average from 69–85% and 80–95% for stations north and south of the Alps, respectively, showing that traffic contributes on average only up to ~30% to OC. The non-fossil fraction of EC ($f_{NF,EC}$), entirely attributable to primary wood burning, was on average 42 ± 13% and 49 ± 15% for north and south of the Alps, respectively. While a high correlation was observed between fossil EC and nitrogen oxides, both primarily emitted by traffic, these species did not significantly correlate with fossil OC (OC_F), which seems to suggest that a considerable amount of OC_F is secondary, from fossil precursors. Elevated $f_{NF,EC}$ and $f_{NF,OC}$ values and the high correlation of the latter with other wood burning markers, including levoglucosan and water soluble potassium (K^+) indicate that residential wood burning is the major source of carbonaceous aerosols during winter-smog episodes in Switzerland. The inspection of the non-fossil OC and EC levels and the relation with levoglucosan and water-soluble K^+ shows different ratios for stations north and south of the Alps, most likely because of differences in burning technologies, for these two regions in Switzerland.

1 Introduction

Ambient particulate matter (PM) influences the Earth's climate directly by scattering and absorbing solar radiation and indirectly by modifying cloud microphysics (Pöschl, 2005; IPCC, 2013). In addition, aerosol particles also adversely affect human health as they can cause respiratory and cardiovascular diseases which can lead to increased mortality (Pope and Dockery, 2006; WHO, 2006). In Alpine regions and most parts of Switzerland elevated PM

concentrations are often found during winter-time since topography (e.g. alpine valleys) and frequent thermal inversions favor the accumulation of pollutants (Gehrig and Buchmann, 2003; Ruffieux et al., 2006). Environmental pollution control strategies and policies have focused mainly on emissions from fossil fuel combustion so far (e.g. road traffic and industry). However, many recent studies have shown that wood burning emissions from domestic heating can be the dominating source of carbonaceous aerosols during the cold season, in Europe (e.g. Szidat et al., 2006; Szidat et al., 2007; Lanz et al., 2008; Favez et al., 2010; Lanz et al., 2010; Gilardoni et al., 2011; Harrison et al., 2012; Herich et al., 2014 and references therein). Therefore, the quantification of the fossil and non-fossil, especially wood burning, contributions to PM, particularly for days with high PM concentrations, is crucial for establishing effective mitigation strategies.

Carbonaceous particles are a major fraction of the fine aerosol ($PM_{2.5}$, PM < 2.5 μm), contributing from 10% up to 90% of the PM mass (Gelencsér, 2004; Putaud et al., 2004; Jimenez et al., 2009). Carbonaceous aerosols are further classified into two sub-fractions: elemental carbon (EC) and organic carbon (OC) (Jacobson et al., 2000). EC originates from incomplete combustion of fossil and non-fossil fuels (e.g. coal, gasoline, diesel, oil and biomass), exclusively emitted directly as primary aerosol in the atmosphere. Meanwhile, OC may be either primary OC (POC) directly emitted in the atmosphere or secondary OC (SOC) formed in the atmosphere through the oxidation of volatile organic compounds (VOCs) from both fossil (coal combustion, industrial and vehicle emissions) and non-fossil (e.g. wood burning and biogenic emissions as well as cooking) sources (Jacobson et al., 2000; Pöschl, 2005; Hallquist et al., 2009). Among several techniques applied to identify and quantify carbonaceous aerosol sources, radiocarbon (^{14}C, half-life = 5730 years) analysis is a quantitative tool for unambiguously distinguishing fossil and non-fossil sources. ^{14}C is completely depleted in emissions from fossil-fuel combustion, which can therefore be separated from non-fossil carbon sources which have a similar ^{14}C signal as atmospheric carbon dioxide (CO_2) (Szidat, 2009; Heal, 2014). The most detailed information about different sources can be achieved when ^{14}C measurements are performed on OC and EC separately, since EC originates exclusively from biomass burning and fossil fuel combustion. By contrast, the apportionment of OC into these two sources using this methodology is less straightforward due to the complex primary and secondary sources of this fraction.

Radiocarbon-based source apportionment results available in the literature are often reported from measurement campaigns covering rather short periods (e.g. several days or a few months, see Hodzic et al. (2010), Minguillón et al. (2011) and Heal (2014) and references therein for a summary of several publications). Very few studies present annual or seasonal results from a full year or several seasons. For example, only two ^{14}C dataset are available covering a time period of two full years (Gelencsér et al., 2007; Larsen et al., 2012), while only a few studies present a yearly cycle (e.g. Huang et al., 2010; Ceburnis et al., 2011; Genberg et al., 2011; Gilardoni et al., 2011; Zhang et al., 2014) or data from two consecutive summers (Tanner et al., 2004) or winters (Glasius et al., 2011). In addition, ^{14}C results from the same time period are available simultaneously only for a limited number of stations (usually less than five, see Heal (2014) and references therein). Furthermore, only a few groups worldwide perform ^{14}C measurements of the EC fraction, since such analyses are still challenging and since there are still open questions concerning the optimal approach for the EC isolation for ^{14}C analysis (Zhang et al., 2012; Bernardoni et al., 2013; Szidat et al., 2013; Dusek et al., 2014). As a consequence, results of ^{14}C measurements carried out separately on EC and OC are still very scarce (see Minguillón et al. (2011) and Heal (2014) and references therein).

In this study, we present, to the best of our knowledge, for the first time ^{14}C measurements covering a time period of five years. Aerosol filter samples were collected during winter-smog episodes (days exceeding the Swiss daily PM_{10} limit of 50 µg m^{-3}), at 16 air pollution monitoring stations across Switzerland to provide a good spatial resolution as well as different source characteristics in various area types (e.g. urban, suburban, rural, alpine valley, traffic, background, etc.). These samples were analyzed for the ^{14}C content in EC and OC, levoglucosan, and major water soluble ionic species. The duration of this project together with the large number of stations results in one of the world's largest aerosol ^{14}C datasets available. This paper is the first paper of a two-part series investigating the spatial and temporal variability in the fossil and non-fossil sources of the organic and elemental carbon during high pollution events in Switzerland. This paper presents the ^{14}C-based source apportionment results of carbonaceous aerosols and investigates their spatial variability. The second paper will explore the influence of meteorological parameters on the different carbonaceous components, their temporal variability and their possible trends in the last years (Zotter et al., 2014).

2 Materials and methods

2.1 Aerosol sampling

The filter samples analyzed in this study were collected at four stations of the Swiss National (NABEL) and 12 stations of the Cantonal air pollution monitoring networks, (EMPA, 2013; Cercl'Air, 2012). These were selected such that a good spatial distribution across Switzerland is achieved (see Fig. 1). In detail, eight stations (PAY, SOL, SIS, BAS, REI, BER, ZUR and STG) are located on the Swiss plateau, one station each in the Rhine and Rhone valley (VAD and MAS, respectively) and one station (SCH) in a small alpine valley in central Switzerland. Those 11 stations will be further referred to as stations "north of the Alps". In addition, five sites "south of the Alps" were selected. These include stations at the Italian boarder where the terrain is more open (e.g. station CHI), plus other stations enclosed within narrow valleys (e.g. stations SVI and ROV). The locations of the stations are shown in Fig. 1 and related details are listed in Table 1. Furthermore, the selection of the stations was also carried out such that the full range of different station characteristics (from urban/traffic to rural background, see Table 1) was covered.

At the selected sites, aerosols were collected onto quartz fiber filters (Pallflex 2500QAT-UP) for 24 h on a regular basis (every 2^{nd} or 4^{th} day or daily depending on the station) using high-volume samplers (Digitel DHA-80, Switzerland) operating at a flow rate of 500 l min^{-1} and equipped with PM_{10} inlets. After the sampling, filters were wrapped in aluminum foil or lint free paper, sealed in plastic bags, and stored at -20°C until analysis. Filter sampling has been widely used but well-known non-systematic artefacts due to adsorption and volatilization of semi-volatile compounds exist (Viana et al., 2006; Jacobson et al., 2000). Since a more complex sampling (e.g. using 2 sampling lines in parallel, one with and the other without a denuder system for volatile OC removal or using 2 filters in series) is not carried out at regular air pollution monitoring stations, artefacts could not be quantified. However, due to the high filter loadings in winter such sampling artefacts are not expected to have a large contribution (e.g. Viana et al. (2007) found a 5% and 7% contribution of OC from positive sampling artifacts for winter samples in Amsterdam and Ghent) and we assume that they will not significantly influence the results presented in this study. It should be noted that on some filters PM_{10} mass was measured gravimetrically which includes weighting before and after the

sampling at a relative humidity (RH) of 50 ± 2% and a temperature (T) of 20 ± 2°C after conditioning for 48 h. Since these handling steps may introduce additional artefacts and none of the samples were pre-heated to remove any OC or EC present on the filters prior to sampling, the analysis of blank filters which were treated exactly the same way as the samples is very important. Therefore, ~50 field blank filters were collected and 34 of them were analyzed for ^{14}C in OC, 45 for major water-soluble ionic species and 47 for OC and EC mass loading.

Every winter, 5 days with high PM_{10} concentrations were investigated and therefore, most of the results presented below are considered as representative for winter-smog episodes, which were the objective of our study. Winter-smog episodes in Switzerland frequently occur on days with inversions, and hence relatively shallow boundary layer heights. The days were selected such that ideally PM_{10} concentrations at all stations exceeded the daily limit value of 50 $\mu g\ m^{-3}$. However, since meteorological conditions in Switzerland north and south of the Alps can differ strongly in winter, it was not possible to find enough days where the selection criterion was fulfilled at all stations simultaneously. Therefore, 5 identical days were chosen separately for stations south and north of the Alps. This ensures similar meteorology and the interpretability of the results in terms of spatial variations within the two regions. In addition, two to three filters per month from August 2008 to July 2009 of the urban background station ZUR were selected to cover a full yearly cycle. In total 320 aerosol filter samples were analyzed for this study. The detailed selection of all analyzed days and the distribution of PM_{10} concentrations on those days for every station are shown in Table S1 in the supporting information and Fig. 2, respectively.

2.2 EC/OC measurements

The EC and OC concentrations were measured on all samples (n = 320) and blanks (n = 47) using a thermo-optical OC/EC analyzer (Model 4L, Sunset Laboratory Inc., USA), which is equipped with a non-dispersive infrared (NDIR) detector. All samples were combusted following the thermal-optical transmittance method (TOT) using the EUSAAR2 temperature protocol (Cavalli et al., 2010). It should be noted here that the OC/EC determination with TOT instruments is not standardized yet and that measurements with different thermal protocols (e.g. NIOSH (NIOSH, 1999; Peterson and Richards, 2002), IMPROVE (Chow et al., 1993), EUSAAR2 (Cavalli et al., 2010)) may lead to discrepancies. Typically, TC measured with different protocols shows good agreement (within 10%), whereas EC can

differ significantly from method to method, up to 25%, and for highly polluted winter samples even up to 60% (Chow et al., 2001, Schmid et al., 2001; Piazzalunga et al., 2011a). We chose the EUSAAR2 protocol since this protocol is also used by the NABEL and Cantonal air quality monitoring programs to measure OC/EC concentrations for some stations on a regular basis.

Repeated measurements were carried out for 150 samples out of the 320. A blank correction was performed using the average TC filter loading (2.5 ± 0.8 μg C cm^{-2}) of all measured blank filters (n = 47) since no systematic differences between the different stations or throughout the years were found (see Fig. S1). Since EC was not detectable in any of the blank samples, the mean TC blank concentration was also used for the blank correction of OC. The average contribution of the blanks to the total filter loading was 5 ± 2% and 4 ± 2% for OC and TC, respectively. The mean measurement uncertainty for OC and TC was estimated to be 7.7% and 8.1%, respectively, using the variability of all samples (n = 8) that were measured three or four times and the variability of the blanks. The uncertainty for EC was assumed to be 25% to account for possible differences between different TOT protocols (Schmid et al., 2001).

2.3 ^{14}C analysis

2.3.1 Separation of carbonaceous particle fractions and ^{14}C analysis

^{14}C analysis of EC and OC was carried out on all samples. ^{14}C content in the blanks was only measured for TC, since an EC loading was not found on those filters (see Sect. 2.2). In the following, we will describe the techniques and procedures of the separation of OC and EC for subsequent ^{14}C measurements.

OC was separated for ^{14}C analysis using the THEODORE system and the Sunset analyzer (see Szidat et al., 2004 and Zhang et al., 2012, respectively for more details). In brief, in THEODORE filter punches with a diameter of 11 to 16 mm were combusted at 340°C for 10 min in a pure oxygen (O_2) stream. The Sunset analyzer, connected to the trapping part of the THEODORE system, was modified such that it could be operated with pure oxygen as a carrier gas in addition to the conventionally used He and He/O_2. The temperatures and combustion times for the oxidation of OC to CO_2 from filter punches with 0.8–1.5 cm^2 in the Sunset analyzer were set to the same values as those used in the THEODORE protocol. The evolving CO_2, from the THEODORE and the Sunset analyzer, was separated from interfering reaction gases, cryo-trapped and sealed in glass ampoules for ^{14}C measurements.

The separation of EC for the ^{14}C measurement was carried out following the Swiss 4S protocol as described by Zhang et al. (2012). First, water-soluble OC (WSOC) and other water-soluble components were removed by water extraction in order to minimize positive artefacts from OC charring (Piazzalunga et al., 2011a; Zhang et al., 2012). The remaining water-insoluble OC (WINSOC) was then removed by a thermal treatment in three steps. In the first two steps, OC was oxidized in O_2 at 375 °C for 150 s and then at 475 °C for 180 s. In the third step, OC was then evaporated in an inert atmosphere in helium at 450 °C for 180 s followed by 180 s at 650 °C. In the end (step four), EC was isolated by the combustion of the remaining carbonaceous material at 760 °C for 150 s in O_2. This method was optimized to reduce biases in ^{14}C measurements of EC related to OC charring (leading to higher non-fossil EC (EC_{NF}) values) or losses of the least refractory EC (mostly from wood burning) during the WINSOC removal (in the steps one to three) as those would lead to lower EC_{NF} fractions. Furthermore, using the Sunset analyzer for the combustion made it possible to quantify those artefacts online, since this instrument monitors the filters during the combustion with a laser. As proposed by Zhang et al. (2012) we tested the effect of different temperatures in step two and three of the thermal protocol on the EC yields and the OC charring for some samples from stations with contrasting sources and filter loadings (e.g. highly and low loaded filters from stations with a large wood burning contribution vs. more traffic influenced stations). Charring of OC most likely occurred only at lower temperature in the steps one and two and was quantified as the difference of the maximum attenuation (ATN) and the initial ATN normalized to the initial ATN of the given thermal step. The EC yield denotes the fraction of EC remaining on the filter samples after the first three OC removal steps before the last step (step four) starts, which was used for the EC recovery for ^{14}C analysis, and is defined as ratio between the initial ATN of the laser signal through the filter before step one of the thermal treatment and the ATN before step four. We found that the EC yield and charring did not vary significantly due to different temperatures (550°C–700°C) in step three and therefore this temperature was set to 650°C as suggested by Zhang et al. (2012). In contrast, varying the temperature in step two we found 525°C and 500°C as optimal values for SVI and BER, respectively, which exhibited very high filter loadings. Higher temperatures for these two stations were necessary to assure complete removal of OC and possibly charred OC before the EC step (step four). For the samples from the other stations 475°C, as suggested by Zhang et al. (2012), was found to be the optimal setting. On average 74 ± 11% of the EC was recovered

for the ^{14}C measurement for all samples and charred OC only contributed 5.3 ± 4.5% to EC recovered in step four.

The ^{14}C measurement of the collected CO_2 from the separated carbonaceous fractions was performed with the **MI**ni radio**CA**rbon **DA**ting **S**ystem, MICADAS (Synal et al., 2007) at the Swiss Federal Institute of Technology (ETH) Zürich and the Laboratory for the Analysis of Radiocarbon with AMS (LARA), University of Bern (Szidat et al., 2014), Switzerland, using a gas ion source (Ruff et al., 2007; Wacker et al., 2013), which allows direct CO_2 injection after dilution with He (Ruff et al., 2010). All ^{14}C results are expressed as fraction of modern (f_M) representing the ratio of the $^{14}C/^{12}C$ content of the sample related to the isotopic ratio of the reference year 1950 (Stuiver and Polach, 1977). The f_M values were corrected for $\delta^{13}C$ fractionation (Wacker et al., 2010) and for the ^{14}C decay between 1950 and the year of measurement. The uncertainty of the measured f_M values for OC and EC ($f_{M,OC}$ and $f_{M,EC}$, respectively) is on average ~2% for the samples presented here.

2.3.2 Data correction and presentation

As discussed in the following, several corrections have to be applied to the f_M values obtained from the ^{14}C measurement (see also Table 2 for a summary).

1) *Blank correction:* A mass-dependent blank correction is applied to the measured f_M values following an isotopic mass balance approach (Zapf et al., 2013):

$$f_{M,corr} = (mC_{sample} * f_{M,\,sample} - mC_{blk} * f_{M,blk}) / (mC_{sample} - mC_{blk}) \quad (1)$$

where $f_{M,corr}$ is the blank corrected f_M, and $f_{M,sample}$ and $f_{M,blk}$ are the f_M measured for samples and blanks, respectively. mC_{sample} and mC_{blk} denote the carbon mass in the samples and the blanks, respectively. Since blank filters are not available for all stations and years and since the ^{14}C results of the blanks were not systematically different (between different stations or years, see Fig. S1), the average f_M and TC values of the blanks, 0.53 ± 0.12 (n = 34) and 2.5 ± 0.8 μgC cm^{-2} (n = 47), respectively, were considered for the correction of $f_{M,OC}$ ($f_{M,OC,corr}$). The blank correction increases the $f_{M,OC,corr}$ values by ~3% and the uncertainty (error propagation of Eq. (1)) rises to ~3%. No EC was detected on the blank filters (see Sect. 2.2 above) and therefore no blank correction was carried out for $f_{M,EC}$.

2) *EC yield correction:* The fraction of EC, which was isolated for the ^{14}C measurement (EC yield) was on average 74 ± 11% as shown in Sect. 2.3.1. However, Zhang et al. (2012) showed that $f_{M,EC}$ changes with different EC recoveries. They found a linear relationship

between $f_{M,EC}$ and the EC yield, which they used to extrapolate $f_{M,EC}$ to 100% EC yield using the average slope (0.31 ± 0.1) from several samples (n = 5) in order to account for the slight underestimation of biomass burning EC caused by the EC loss during EC isolation for ^{14}C measurement (see Sect. 2.3.1 above). In this study, we also measured $f_{M,EC}$ from 11 samples at different EC yields. As shown in Fig. S2 there is also a linear relationship between the EC yield and $f_{M,EC}$ for the samples from this study. Even though the slopes exhibit a larger variability compared to the ones presented in Zhang et al. (2012) the average slope of all winter samples is very similar. In contrast, the slopes for the summer filters show only a very weak relationship between $f_{M,EC}$ and the EC yield due to the smaller fraction of less refractory EC (mainly from biomass burning) which is removed before the EC isolation for the ^{14}C analysis. Beside the clear difference between samples from summer and winter, no systematic differences between different stations or years were found. Therefore, average slopes of 0.35 ± 0.11 and 0.07 ± 0.03 for winter and summer samples, respectively, were taken to correct all $f_{M,EC}$ values to 100% EC yield ($f_{M,EC,total}$) using the following equation (Zhang et al., 2012):

$$f_{M,EC,total} = slope * (1 - EC_{yield}) + f_{M,EC} \quad (2)$$

The uncertainty of $f_{M,EC,total}$ was obtained by an error propagation of Eq. (2) using the variability of the average slopes, the measurement uncertainty of $f_{M,EC}$ and an assigned uncertainty of 10% for the EC yield and is on average 4.2 %.

3) *Charring correction:* Approximately 50 samples exhibited OC charring contributing >10% to EC even though the method used here for EC isolation is optimized to minimize OC charring. Therefore, the $f_{M,EC,total}$ values were corrected for charring ($f_{M,EC,final}$) using the same isotopic mass balance approach as described in Eq. (1) in which the f_M and mC values of the samples and blanks were replaced by $f_{M,EC,total}$ and EC as well as the fraction (f_{charr}, formed in step one and two of the thermal treatment as described in 2.3.1) and f_M of charred OC ($f_{M,charr}$). We assumed that only 50% of the charred OC contributed to the ^{14}C result of EC since some charred material was most likely removed in step three. However, since some EC could be lost in step three as well the charred OC evaporated in step three cannot be quantified. Therefore, a high uncertainty of 33% is assigned to the fraction of charred OC which should in addition account for possible differences and variability between samples and stations. The $f_{M,charr}$ was obtained from ^{14}C measurements (n = 11) of WINSOC from water-extracted filters released in step one and was found to be on average 0.78. To account for possible sample-to-sample differences and variability between samples and stations we

assigned an uncertainty of 0.10 for $f_{M,charr}$. The uncertainty of $f_{M,EC,final}$ was on average 4.4%, which is only slightly higher than for $f_{M,EC,total}$ (4.2%).

4) *Bomb peak correction:* Samples from fossil sources are characterized by $f_M = 0$ due to the extinction of ^{14}C with a half-life of 5730 years whereas f_M is equal to one for contemporary carbon sources including biogenic and biomass burning ($f_{M,bio}$ and $f_{M,bb}$, respectively). However, due to the thermonuclear weapon tests of the late 1950s and early 1960s the radiocarbon content of the atmosphere increased and f_M exhibit values greater than one (Levin et al., 2010). To account for this effect, the $f_{M,OC,corr}$ and $f_{M,EC,final}$ values are converted into non-fossil fractions ($f_{NF,OC}$ and $f_{NF,EC}$, respectively) (Szidat et al., 2006; Zhang et al., 2012) using a reference value ($f_{NF,ref}$) representing the modern ^{14}C content during the sampling period compared to 1950 before the bomb testing. EC is only emitted from fossil sources or biomass burning (neglecting any EC emissions from biofuels as their contribution to the total fuel use is low). Hence, $f_{NF,ref}$ equals $f_{M,bb}$ to correct $f_{M,EC}$ whereas it includes additionally $f_{M,bio}$ and the fraction of biogenic sources to the total non-fossil sources (p_{bio}) for the calculation of $f_{NF,OC}$. $f_{M,bio}$ was taken from long-term $^{14}CO_2$ measurements at the background station Schauinsland (Levin et al., 2010) and $f_{M,bb}$ was estimated using a tree growth model as described in Mohn et al. (2008). p_{bio} was set to 0.2 ± 0.2 since no large contributions from biogenic sources are expected in Switzerland during winter-smog episodes. In any case, p_{bio} has only a very little impact on $f_{NF,ref}$ compared to other measurement uncertainties (e.g. an increase of p_{bio} from 0.2 to 0.4 would change $f_{NF,ref}$ for this study only by max. 1.8%). The $f_{M,bio}$, $f_{M,bb}$ and $f_{NF,ref}$ values for the different years, which were consequently used to determine $f_{NF,\,OC}$ and $f_{NF,\,EC}$, are shown in Table S3. The final uncertainties for $f_{NF,OC}$ and $f_{NF,EC}$ (~3 % and ~5 %, respectively) were derived from an error propagation and include all the individual uncertainties of the f_M values, $f_{M,bio}$, $f_{M,bb}$ and p_{bio}.

2.4 Analyses of water-soluble major ionic species and levoglucosan

The concentrations of major water-soluble ionic species (cations: K^+, Na^+, Mg^{2+}, Ca^{2+} and NH_4^+; anions: methanesulfonate (MSA), oxalate (Ox^{2-}), SO_4^{2-}, NO_3^- and Cl^-) were analyzed on all filters (n = 320) and field blanks (n = 45) with an ion chromatographic system (850 Professional, Metrohm, Switzerland) equipped with a Metrosept C4 cation column and a Metrosept A anion column, respectively. Prior to the measurement a water extraction (15 ml and 50 ml for samples from 2008-2010 and 2011-2012, respectively) with ultrapure water

(18.2 MΩ cm^{-1}) for 30 min at 40 °C in an ultrasonic bath of filter punches with a diameter of 11 mm was carried out. The measurement uncertainty for most of the water-soluble ions was estimated to be 10%. An uncertainty of 30% was assigned for all cations as well as for Ox^{2-} and Cl^- with concentrations < 5 ppb in solution. A blank correction was carried out subtracting an average value of each ionic species from the concentrations in the samples. In contrast to the blank correction of the OC and TC concentrations as well as $f_{NF,OC}$, where an average value of all blanks (different stations and years) was used, the average of all blanks from the different stations from each winter was taken separately. It should be noted here that not all ionic species were detected in all blanks (see Fig. S1 and Table S2). The overall uncertainty of the major water-soluble ionic species was derived from the error propagation of the measurement uncertainty and the blank variability.

Levoglucosan was measured following the procedures described in Piazzalunga et al. (2010) and (2013a). In brief, levoglucosan was measured by a high-performance anion-exchange chromatography (HPAEC) with pulsed amperometric detection (PAD) using an ion chromatograph (Dionex ICS1000) equipped with an isocratic pump and a sample injection valve with a 100 μL sample loop. Prior to the analysis, a water extraction was carried out by three subsequent extractions of ~2 cm^2 filter punches by 20-min sonication using 2 mL Millipore-MilliQ water (18.2 MΩ cm^{-1}). Levoglucosan was then separated from other compounds by a Carbopac PA-10 guard column (50 mm×4 mm) and a Carbopac PA-10 anion exchange analytical column (250 mm×4 mm) using 18 mM NaOH as an eluent. The analytical system comprised an amperometric detector (Dionex ED50) equipped with an electrochemical cell. The detector cell had a disposable gold electrode and a pH electrode as reference (both from Dionex) and was operated in the pulsed amperometric detection (PAD) mode. The measurement uncertainty was estimated to be ~5% using the average repeatability of several standards and the limit of detection in solution is 2 ppb. The levoglucosan concentrations were also analyzed for blank filters but were below the detection limit and therefore no blank correction was performed.

2.5 Additional data

Since all sampling sites in this project are part of the Swiss national (NABEL) or cantonal air pollution monitoring networks, additional parameters (e.g. gas phase pollutants, particle mass and meteorology) are routinely measured. PM_{10} and nitrogen oxides (NO_x = NO and NO_2)

data are available from all stations (except SCH), whereas ozone (O_3), sulfur dioxide (SO_2) and carbon monoxide (CO) measurements are only performed at some stations. Reference instrumentation according to the valid European standards was used. PM_{10} is measured online with beta attenuation monitors (FH62-IR, Thermo ESM Andersen) and by TEOM-FDMS (Thermo Environmental) instruments and an approach presented in Gehrig et al. (2005) to correct/harmonize online and gravimetric PM_{10} measurements is routinely applied to data from all stations. It should be noted that NO_x measurements using molybdenum converters suffer from interference of oxidation products of NO_x which is however not crucial for winter-time conditions (Steinbacher et al., 2007). The meteorological parameters wind-speed, wind-direction, temperature (T), relative humidity (RH), precipitation and global radiation were also only measured at some of the sites. For the remaining sampling locations meteorological data were taken from nearby stations operated by the Swiss weather service (MeteoSwiss, 2014). In all networks (NABEL, Cantons and MeteoSwiss) data sets (except results obtained offline from filter samples, i.e. EC/OC and levoglucosan concentrations as well as ^{14}C data) undergo an automatic and a manual quality check (data should be (1) within a plausible range, (2) show plausible variability, (3) reproduce to a reasonable extent the expected daily, monthly and yearly variations, (4) whenever possible measurements are compared to nearby or similar stations with the expectation of similar values (Barmpadimos et al., 2011)).

3 Results and discussion

3.1 Composition of PM_{10}

As we were interested in winter-smog episodes only days with high PM_{10} concentrations at all stations were analyzed. As shown in Fig. 2a the selected days from almost all locations exhibited on average values ~50 μg m^{-3} (European and Swiss daily limit) or above. While not exactly the same days were chosen for stations north and south of the main chain of the Alps, it is nevertheless evident that the PM_{10} burden during winter-smog episodes in Switzerland is higher south of the Alps (73 ± 27 μg m^{-3} in the south compared to 55 ± 16 μg m^{-3} in the north). These episodes often occur in winter during stable meteorological conditions including periods with high pressure, rather low temperatures and weak winds (typically less than 2 m s^{-1}). Such conditions often lead to inversions with low mixing layer heights, thereby favoring

the accumulation of pollutants and consequently causing high PM_{10} concentrations. The reason for the higher PM_{10} values at stations south of the Alps is most likely due to a combination of topography (e.g. several stations are located in alpine valleys), local meteorology (e.g. more persistent inversions with rather low mixing heights compared to the north) and emissions (strong local wood burning influence, see Sect. 3.2.1 and 3.2.2 below).

As only 5 winter-smog-episode days from each of the 5 winter seasons were selected and to account for possible differences in the concentration levels between the stations (especially locations north vs. south of the Alps), we will mainly focus here on the fractional contributions of the individual compounds to total PM_{10}. The major water-soluble ions, EC and OM measured here explain 82 ± 11% of the total PM_{10} mass. The missing fraction could mostly be attributed to aerosol water content, the water insoluble fraction (e.g., dust particles), and/or to the uncertainties of the different measurement methods and OM:OC ratio used to convert OC to OM. The major contributors to PM_{10} during winter-smog episodes in Switzerland were on average the organic matter (OM = OC * 1.8, Turpin and Lim, 2001), with 29 ± 7% and 46 ± 17% followed by the secondary inorganic aerosol (SIA) constituents nitrate (NO_3^-, 25 ± 9% and 20 ± 11%), sulfate (SO_4^{2-}, 10 ± 4% and 6 ± 3%) and ammonium (NH_4^+, 9 ± 3% and 7 ± 4%) for stations north and south of the Alps, respectively (see Fig. 2). Differences observed in the chemical composition of the aerosol between south and north are a first indication that different emission sources may dominate the aerosol burden at these locations. The EC shares of PM_{10} were on average 4 ± 2% in the north and 6 ± 3% in the south.

For stations north of the Alps, the range of OM contribution is rather stable (station averages 23–32%), whereas south of the Alps, OM fraction span a wider range (station averages 35–52%), with values statistically significantly higher than in the north (t-test significant at 95%, in general throughout the manuscript we always used a t-test with $p = 0.05$ to test the statistical significance of differences between stations north and south of the Alps). Furthermore, a clear trend towards larger OM contributions at more rural stations is evident in the south. The EC shares of PM_{10} are on average slightly lower in the north compared to the south but show similar variations among the different stations (averages range between 3–5% in the north and 5–7% in the south). As already shown above the contributions of the different SIA components to PM_{10} are larger in the north. In addition, they also show larger station-to-station differences (averages range from 9–30% for NO_3^-, 5–11% for NH_4^+ and 7–12% for

SO_4^{2-} in the north compared to 14–24% for NO_3^-, 5–8% for NH_4^+ and 5–6% for SO_4^{2-} in the south). While almost all constituents of PM_{10} (OM, EC and NO_3^-) exhibit on average larger concentrations in the south (mainly due to the selection of days with higher PM_{10} concentrations compared to the ones selected in the north), NH_4^+ shows on average very similar levels in both regions and SO_4^{2-} even higher ones in the north (see Fig. S3). The higher SO_4^{2-} fractions and levels observed north of the Alps indicate a higher background of this species possibly caused by occasional long-range transport of SO_2 emissions from Eastern Europe. Another interesting feature is evident for the stations south of the Alps. The relative contributions of NO_3^- and NH_4^+ exhibit a trend towards lower values at rural stations, as opposed to the OM fraction (see Fig. 2), which may be due to the influence of the stations in the south by air masses advected from the Po Valley, where emissions from fossil fuel combustion (e.g. NO_x) are elevated (Piazzalunga et al., 2011b; Larsen et al., 2012) compared to the southern part of Switzerland. More details about the influence of air masses originating from other regions outside Switzerland will be discussed in Zotter et al. (2014).

3.2 ^{14}C–based source apportionment

3.2.1 Relative fossil and non-fossil contributions of OC and EC

Figure 3 summarizes the individual results of all ^{14}C measurements (n ~ 300 for OC and EC) from all stations for the 5 winters (2007/2008–2011/2012), except for REI, MOL, ROV and SCH (one winter) and BAS (two winters), as noted in Table 2. The use of Whisker boxplots enables the identification of the variability of the results for each station as well as the station-to-station differences. Several filters from BAS showed clearly elevated $f_{NF,OC}$ values (larger than one and up to five) indicating that BAS is influenced by sources emitting anthropogenic ^{14}C (e.g. from nuclear power plants, pharmaceutical industry and biochemical laboratories working with labeled ^{14}C, incinerators for medical waste). BAS is the base for two of the world's largest pharmaceutical enterprises, Roche and Novartis, and in addition an incinerator for medical waste is located in the vicinity of the station. Furthermore, ^{14}C measurements on leaf samples across the city of Basel also showed partially highly elevated results (BAG, 2008), indicating ^{14}C-enriched CO_2. Therefore, $f_{NF,OC}$ values from BAS were not considered for the further analysis. This artefact is however restricted to OC; the $f_{NF,EC}$ results did not show such an influence (see Fig. 3b) and are included and discussed throughout this study.

The data from the yearly cycle in ZUR is also excluded here but will be investigated in part II (Zotter et al., 2014).

The range of all $f_{NF,OC}$ values (except BAS) as displayed in Fig. 3a is 0.59–0.95 and 0.62–1.02 for stations north and south of the Alps, respectively. A few samples (n = 4) with $f_{NF,OC}$ values slightly above one were found in SVI and are within the uncertainty (~3%) of $f_{NF,OC}$. They can be explained on the one hand with very high local wood-burning contributions and on the other hand with the uncertainties in the reference value $f_{NF,ref}$ used for the correction of the still elevated ^{14}C concentrations due to the above-ground thermo-nuclear bomb tests (see Sect. 2.3.2). The average $f_{NF,OC}$ values for stations north and south of the alps are 0.78 ± 0.08 (median = 0.78) and 0.82 ± 0.07 (median = 0.83), respectively, showing that on average locations south of the Alps are more impacted by non-fossil sources. As discussed above, non-fossil OC may include, POC and SOC from wood burning and cooking emissions, as well as primary biological particles and biogenic SOC. Cooking was estimated to contribute on average only 7.5% to OA during winter in ZUR which is the largest city of Switzerland (Canonaco et al., 2013), and is therefore expected to contribute less at the other stations. Furthermore, large inputs from biological and biogenic sources are also not expected under Swiss winter conditions, characterized by low biological activity. Therefore, the high $f_{NF,OC}$ values indicate that wood burning POC and SOC are most probably the main source of OC during winter-smog episodes in Switzerland. The highest $f_{NF,OC}$ values north and south of the Alps were found at the rural stations SCH (0.85 ± 0.04) and SVI (0.95 ± 0.05), which are located in narrow alpine valleys. The lowest non-fossil contributions to OC were observed in BER, STG, VAD and ZUR north of the Alps as well as in MOL and CHI south of the Alps, but were on average never below 70% showing that sources of fossil carbon only account for a small fraction of OC during winter-smog episodes in Switzerland, even at urban and traffic-influenced stations. Furthermore, the variability of all $f_{NF,OC}$ values for the individual stations and the station to station differences (with the exception of SVI and BER which present the highest and lowest values, respectively) are low as displayed by the small interquartile ranges (IQR = 3^{rd} – 1^{st} quartile; 0.10 ± 0.02 in the north and 0.08 ± 0.02 south of the Alps) and the small range of the station averages (0.75–0.85 and 0.80–0.86 for stations north and south of the Alps, respectively). This suggests that the relative source contributions to OC are very consistent within Switzerland during winter-smog episodes.

Similar high non-fossil contributions to OC were also found in previous studies in Switzerland. The $f_{NF,OC}$ values for ZUR, ROV, MOL, REI and Sedel as well as MAS, Saxon, Sion and Brigerbad ranged on average from 61–76% with values above 90% in ROV (Szidat et al., 2006; Szidat et al., 2007; Sandradewi et al., 2008a and 2008b; Perron et al., 2010). Results previously reported for other regions in Europe show lower biomass burning contributions to OC: e.g. biomass burning OC (OC_{BB}) to the total OC fraction of 35–54% at three Austrian cities (Vienna, Graz and Salzburg, Caseiro et al., 2009), 28–65% at three locations in the Po Valley (Milan, Sondrio and Ispra, Gilardoni et al., 2011; Piazzalunga et al., 2011b) and 60% in Grenoble (Favez et al., 2010).

The non-fossil fraction of EC relate more unambiguously to wood burning. For most stations the wood burning contribution was found to be <50% and thus the contribution from fossil fuel combustion, mostly due to traffic, was >50% (see Fig. 3b). However, since the average $f_{NF,EC}$ values, except for BER, REI and MOL, never decrease below 0.4, it is evident that wood burning emissions exceptionally account for a large fraction of EC during winter-smog episodes in Switzerland. The individual $f_{NF,EC}$ values range from 0.12–0.79 (on average 0.42 ± 0.13) and 0.25–0.87 (on average 0.49 ± 0.15) for all stations north and south of the Alps, respectively, showing that for EC the contributions from wood burning are higher for locations south of the Alps. The lowest $f_{NF,EC}$ values were found at the stations BER (0.22 ± 0.06), MOL (0.28 ± 0.06) and REI (0.35 ± 0.05), which are directly exposed to traffic emissions from nearby roads with a high traffic flow. Extremely high non-fossil contributions to EC up to 87% and 79% were observed in SVI (66 ± 11%) and SCH (69 ± 9%). Both stations are located in narrow alpine valleys characterized by frequent winter-time inversions and are strongly influenced by local emissions from wood combustion, which is the main source for residential heating in such areas in Switzerland.

Elevated non-fossil contributions to EC have already been observed during previous campaigns in Switzerland (71 ± 18% and 84 ± 13% on average in ROV and individual results between 60% and 70% in MAS, PAY, Sedel, Brigerbad, Saxon and Sion, see Zhang et al. (2012) and references therein). Similar $f_{NF,EC}$ results were previously also reported for ZUR (0.24–0.34), BER (0.14), BAS (0.30), MAG (0.30–0.56), MOL (0.24), PAY (0.33–0.43) and REI (0.37) (see Zhang et al. (2012) and Herich et al. (2014), and references therein). $f_{NF,EC}$ for stations on the Po-valley (0.16 in Milan, 0.29 in Sondrio and 0.49 in Ispra, Gilardoni et al., 2011; Piazzalunga et al., 2011b) and Grenoble (0.17, Favez et al., 2010) are comparable as

well, whereas for two urban stations in Sweden (Gothenburg and Stockholm) a wide range for $f_{NF,EC}$ was found (0.12–0.88, Zencak et al., 2007 Szidat et al., 2009; Andersson et al., 2011).

The most prominent feature in Fig. 3 is the clear non-fossil increase south of the Alps from MOL to SVI for OC and EC. With the exception of MOL, which is directly located next to a highway, these stations are not only ordered from the most urban and traffic influenced to the most rural, but also geographically from south to north. CHI is located in a more open terrain at the Swiss/Italian border, whereas further north, towards the main Alpine chain, narrower alpine valleys dominate and the region is consequently more rural and wood burning for wintertime residential heating becomes more important. The observation that the non-fossil contributions for both, OC and EC, are on average higher at locations south of the Alps can thus be mainly attributed to the fact that there are more rural stations in the south whereas urban and suburban stations dominate north of the Alps (see Fig. 1).

3.2.2 Total fossil and non-fossil contributions

Next we will discuss the fossil and non-fossil concentrations of OC and EC and their contributions to TC. The fraction of TC in PM_{10} is on average 19–25% for stations north of the Alps and is slightly higher for locations in the south (27–30%). Fig. 4 shows the average EC_F, EC_{NF}, OC_{NF} and OC_F concentrations as well as their relative contributions to TC for all analyzed winter samples for each station. It is evident that sources of non-fossil carbon dominate TC at locations north and south of the Alps with contributions around 70 ± 18% and 79 ± 10% (sum of EC_{NF} and OC_{NF}), respectively. Compared to other winter measurements across Europe this is rather at the higher end of the reported range and higher than reported for urban sites around the world but similar to values found for suburban and rural locations in the US and India (Hodzic et al., 2010; Heal, 2014).

OC_{NF} is the largest fraction of TC, accounting on average for 61 ± 8% and 69 ± 9% for stations north and south of the Alps, respectively, whereas EC_{NF} contributes on average ~9% to TC in both regions of Switzerland. The fossil shares in the north of OC (18 ± 6%) and EC (13 ± 6%) are higher compared to those in the south (OC_F/TC = 12 ± 6% and EC_F/TC 10 ± 5%). The lowest and highest fossil contributions to TC (sum of EC_F and OC_F) were found in SVI (10 ± 6%) and BER (43 ± 7%), respectively. For the stations south of the Alps, a clear decreasing trend in the relative contribution of fossil OC and EC from more traffic to more rural influenced stations is found (see Fig. 4 and Fig. S4). North of the Alps, such a trend is

only evident for EC_F. Relative and absolute non-fossil OC and EC contributions in the north (except BER and SCH which present the highest and lowest values) only show low station-to-station differences (station averages range from 58–71% and 1.5–2.5 µg C m^{-3} for OC_{NF} as well as 8–11% and 0.9–1.9 µg C m^{-3} for EC_{NF}, see Fig. 4 and Fig. S4). In addition, also the variability of the relative and absolute OC_{NF} and EC_{NF} contributions at the individual stations north of the Alps is rather small as evidenced by low IQRs (2.8 ± 0.9 µg C m^{-3} and 7 ± 2% for OC_{NF} as well as 0.4 ± 0.1 µg C m^{-3} and 3 ± 1% for EC_{NF}). Together with the low station-to-station differences, this suggests that non-fossil sources very consistently influence stations on the Swiss Plateau. Furthermore, as discussed above, OC_{NF} can be influenced by SOC formation which can be highly variable. However, the low OC_{NF} station-to-station and day-to-day variability points to a similar degree of atmospheric processing and SOC formation for the chosen days in this region of Switzerland. Last, the low absolute and relative EC_{NF} and OC_{NF} IQRs at the individual stations and station-to-station differences also indicate that locations on the Swiss Plateau are rather influenced by regional (still mainly within Switzerland) air pollution. This is confirmed by high correlations (r = 0.7 ± 0.2, 0.5 ± 0.3, 0.9 ± 0.1 and 0.7 ± 0.1) between the concentrations of EC_F, EC_{NF}, OC_F and OC_{NF} for all measured values from each station located on the Swiss plateau (see Table 1) against ZUR which was chosen as a reference for this region. Furthermore, this is in agreement with Gehrig and Buchmann, 2003) who previously found that (1) under high pressure conditions inversions can extend over the entire Swiss Plateau and typically last several days possibly causing smog formation and (2) that PM concentrations were strongly influenced by meteorology (dilution with clean air or precipitation) rather than by variation of source activities. In contrast, correlating the fossil and non-fossil concentrations of OC and EC from stations south of the Alps against the ones from MAG shows lower values (r = 0.3 ± 0.2, 0.6 ± 0.3, 0.4 ± 0.3 and 0.3 ± 0.3 for OC_{NF}, EC_{NF}, EC_F and OC_F, respectively) indicating that local sources are more important for stations south of the Alps.

3.3 Sources and behavior of fossil and non-fossil organic carbon

3.3.1 Fossil fraction

Fig. 5 presents the comparison between EC_F, OC_F and NO_x, which are expected to be associated with traffic emissions, in Switzerland. EC_F, which is emitted as primary aerosol from vehicles, exhibits a high correlation with NO_x for the stations north (r = 0.79) and south

(r = 0.75) of the Alps, with similar slopes and axis intercepts for both regions (0.021 and 0.015 µg C m^{-3} ppb^{-1} and 0.35 and 0.89 µg C m^{-3} for north and south of the Alps, respectively (see Fig. 5c), indicating a rather similar fleet composition in the two areas. Similar slopes (0.05, 0.03 and 0.02 µg C m^{-3} ppb^{-1}) have been reported previously for 3 locations in Switzerland (MAG, ZUR and PAY, Herich et al., 2011), Grenoble (Favez et al., 2010) and London (Liu et al., 2014). In contrast, no correlation is found between OC_F and the primary vehicular markers, EC_F and NO_x ($r < 0.5$, see Fig. 5b) for stations both north and south of the Alps. Further, the amounts of fossil organic carbon measured are significantly higher than amounts expected for traffic emissions; i.e. observed average $OC_F/EC_F = 1.54 \pm 0.83$ vs. traffic OC/EC = 0.25–0.80 (El Haddad et al., 2013 and references therein). Taken together these observations indicate that a considerable amount of OC_F is associated with emissions or atmospheric pathways that yield organic aerosol with little or no EC_F and NO_x. These processes may include primary emissions from non-mobile fossil fuel combustion sources, e.g. heavy fuel combustion (e.g. crude oil, not widely used in Switzerland), or secondary organic carbon formed from fossil VOCs emitted from traffic.

3.3.2 Non-fossil fraction

As mentioned above a significant fraction of non-fossil carbon during winter-smog episodes originates from wood burning. The use of a single or a set of source specific compound markers from wood burning emissions is often applied to estimate the contribution of this source to ambient aerosol (Herich et al., 2014 and references therein). The most widely used tracer compound for biomass-burning emissions is levoglucosan (Simoneit et al., 1999; Puxbaum et al., 2007; Viana et al., 2013), a product of cellulose combustion. Another wood burning tracer is water-soluble potassium (K^+), which is an inorganic compound mainly present in ash. The wide variability of levoglucosan emission ratios results in significant uncertainties in estimating wood burning contributions. For example, ratios of OC and EC to levoglucosan for alpine regions were reported in Schmidl et al. (2008) to range from 3.7 to 12.5 and from 0.7 to 4.7, respectively, dependent on the combustion conditions and fuel type used (Engling et al., 2006; Lee et al., 2010). Here, we examine the relationship between different measured wood burning markers and the measured OC_{NF}, to investigate the main emission sources and chemical characteristics of this fraction.

The comparison of EC_{NF} and OC_{NF} with levoglucosan (see Fig. 6) shows a high correlation for both species with the latter. The small intercept (1.3 and 2.3 µg C m^{-3} for stations north

and south of the Alps, respectively) and the high correlation ($r > 0.87$) between OC_{NF} and levoglucosan suggests that the majority of OC_{NF} originates from wood combustion; i.e. cooking and, biogenic emissions seem to be minor contributors (see Sect. 3.2.1 above). Furthermore, this indicates that OC_{NF} is to a large extent emitted as primary aerosol, however, with the data presented in this study it is not possible to quantify a primary vs. secondary fraction of wood-burning OC. OC_{NF} also exhibits a high correlation with K^+ as well ($r = 0.62$ in the north and $r = 0.87$ in the south, see Fig. 8a). However, K^+ is also found in soil dust and sea salt or can be formed in incinerators and during meat cooking (Schauer et al., 1999; Schauer et al., 2001), and therefore cannot be used as unambiguous tracer for wood burning, although none of these sources are expected to have a large influence in Switzerland during winter. Another indication for OC_{NF} originating to a large extent from wood combustion is its high correlation ($r = 0.77$, see Fig. 7) with EC_{NF}, which can be almost exclusively attributed to this source.

A high correlation is also found between levoglucosan and K^+ ($r > 0.6$). However, clearly different slopes (0.6 and 5.4) are observed for stations north and south of the Alps, respectively. Furthermore, also the comparison of OC_{NF} and EC_{NF} with levoglucosan as well as OC_{NF} with K^+ shows significantly different ratios for stations located in the north and the south. These discrepancies between the two Swiss regions could originate from different wood types used (e.g. soft and hard wood), burning conditions, and atmospheric processing. Different ratios of OC_{NF} and EC_{NF} to levoglucosan indicate differences in SOC formation and/or photochemical degradation of the latter which was recently reported by Kessler et al. (2010) and Hennigan et al. (2011). However, under winter-smog conditions in Switzerland (low temperatures and photochemical activity) rapid levoglucosan degradation is not expected and no large systematic differences in the photochemical activity and SOC formation between locations south and north of the Alps were found as evidenced by very similar OC_{NF} to EC_{NF} ratios (7.7 ± 2.1 and 8.6 ± 2.9, see Table 3 and Fig. 7) for these two regions in Switzerland. However, with our data we cannot completely rule out different wood burning OC/EC emission ratios in both regions of Switzerland as higher primary wood burning OC emissions in the south could be compensated by a larger non-fossil SOC fraction in the north. Higher ratios of OC_{NF} and levoglucosan to K^+ in the south show that wood burning emissions contain a higher fraction of OC compared to the north. Data from the Swiss forest inventory (Swiss Federal Statistical Office, 2014) show that the fraction of soft (25%) and hard woods (75%) in the energy wood production is very similar between the Swiss Plateau and the regions south

of the Alps (max. 16% difference for the years 2008–2012) suggesting that households in both regions have similar access to soft and hard woods. Therefore, the different ratios between OC_{NF} and K^+ as well as levoglucosan and K^+ are most likely due to different burning conditions. Previous studies demonstrated that particulate emissions from biomass combustion with high temperatures (e.g. in large combustion units, modern stoves and boilers) consist predominantly of inorganic material (K-salts) and contain little OC (Valmari et al., 1998; Johansson et al., 2003; Khalil and Rasmussen, 2003; Heringa et al., 2011; Schmidl et al., 2011). Consequently, dissimilar levoglucosan to K^+ ratios measured at different locations have already been used as indication for different burning conditions in recent studies (Sandradewi et al., 2008b; Caseiro et al., 2009; Piazzalunga et al., 2013b). The lower levoglucosan to K^+ ratios found in this study for locations north of the Alps therefore suggest a larger fraction of more efficient wood burners (e.g. pellet and wood chip burners) in this region compared to the south where wood stoves seem to be operated at rather poor combustion conditions with high carbonaceous and thus lower relative K^+ emissions.

The discussions above clearly showed the differences in wood burning marker ratios at locations north and south of the Alps. However, a closer inspection of the results of Table 3 reveals that most wood burning marker ratios at the stations PAY and MAS (both north of the Alps) are rather similar to the average over all locations south of the Alps and the urban station CHI exhibits values more similar to the average in the north than to the other southern locations. Since in the north mainly urban and suburban stations and south of the Alps mostly rural and/or background sites were chosen (see Table 1 and Fig.1), this suggests that the differences in the wood burning marker ratios between these two Swiss regions are most likely associated with the different station characteristics (e.g. rural and/or background with high wood burning influence vs. urban, suburban and more traffic influenced stations) rather than due to their geographical location within Switzerland.

3.3.3 Comparison of wood burning marker ratios with other studies

Herich et al. (2014) presented an overview about previous studies carried out during winter in Switzerland and other alpine regions in Europe. Several source apportionment methods (including ^{14}C analysis, aethalometer model, positive matrix factorization, chemical mass balance, macro tracer approach, see Gianini et al. (2013) and Herich et al. (2014) for a discussion about possible differences in the biomass burning marker ratios due to different approaches) were used in these studies to estimate the wood burning fraction of OC and EC.

In the following we will compare our biomass burning marker ratios with the ones summarized by Herich et al. (2014). It should be noted that the results presented in the latter study were mainly obtained from short campaigns in just a single winter season and at a limited number of stations, whereas here we performed measurements on winter filters from five years and 16 stations.

The average EC_{NF} to levoglucosan ratio for several stations north of the Alps (BER, PAY, STG, ZUR, REI, BAS, Ebnat-Kappel) from earlier winter measurements in Switzerland is consistent with the results obtained here, but for some southern stations (MAG, MOL, ROV) it is slightly higher than the average ratio found here (see Table 3). EC_{NF}/levoglucosan ratios for three Austrian cities (Vienna, Graz and Salzburg, Caseiro et al., 2009) and three locations in the Po Valley (Milan, Sondrio and Ispra, Gilardoni et al., 2011; Piazzalunga et al., 2011b) which can be considered as north and south of the main chain of the Alps, respectively, exhibit also similar values as those obtained here. Generally lower biomass burning OC (OC_{BB}) to levoglucosan and OC_{BB} to EC_{NF} ratios for the Swiss, Po-valley and Austrian sites located north and south of the Alps were found in Herich et al. (2014) compared to OC_{NF} to levoglucosan and OC_{NF} to EC_{NF} ratios presented here (see Table 3). The differences in the ratios most likely originate from (1) uncertainties in the OC_{BB} determination (e.g. OC/levoglucosan emission ratios have to be assumed which can be highly variable) (2) SOC from wood burning is not taken into account in the OC_{BB} values as presented in Herich et al. (2014) but is included in OC_{NF} as obtained by the ^{14}C measurement and (3) a contribution of other non-fossil sources (e.g. cooking or biogenic aerosol) to OC_{NF} as apportioned with the ^{14}C analysis cannot be completely ruled out although they are expected to have no large influence during winter-smog episodes in Switzerland (see discussion in Sect. 3.2.1 above).

The differences in the wood burning marker ratios between locations north and south of the Alps is also evident for the results presented in Herich et al. (2014). OC_{BB} and EC_{NF} to levoglucosan ratios are higher in the north which was also shown for the same ratios obtained here. In addition, OC_{BB}/EC_{NF} previously found for stations north and south of the Alps in Switzerland are very similar confirming the findings from above (see Sect. 3.3.2) that there is no significant difference in the non-fossil SOC formation between these two regions.

4 Conclusions

In this study we present source apportionment results of winter-smog episodes in Switzerland (days exceeding the Swiss and European daily PM_{10} limit of 50 µg m^{-3}) using radiocarbon (^{14}C) analysis separated for the elemental (EC) and organic (OC) carbon fraction together with levoglucosan, major water-soluble ionic species and gas phase pollutant measurements. Overall, ~300 filter samples from 5 winter seasons (2008-2012) from 16 air pollution monitoring stations across Switzerland with different characteristic (e.g. urban, suburban, rural, alpine valley, traffic, background, etc.) were analyzed providing one of the world's largest aerosol ^{14}C datasets.

The most important contributions to PM_{10} during winter-smog episodes in Switzerland were on average the organic matter OM (29 ± 7% and 46 ± 17%), followed by the secondary inorganic constituents nitrate (NO_3^-, 25 ± 9% and 20 ± 11%), sulfate (SO_4^-, 10 ± 4 % and 6 ± 3%) and ammonium (NH_4^+, 9 ± 3% and 7 ± 4%) for stations north and south of the Alps, respectively. The EC shares of PM_{10} were on average 3–5 % north of the Alps and 5–7% south of the Alps. PM_{10} and OM concentrations during winter-smog episodes in Switzerland were significantly higher for stations south of the Alps, which is most likely due to a combination of topography (e.g. several stations are located in alpine valleys), local meteorology (e.g. more persistent inversions with rather low mixing heights compared to the north) and emissions (strong local wood burning influence).

The fractional non-fossil contribution of organic carbon ($f_{NF,OC}$) determined with the ^{14}C analysis ranges on average between 0.69–0.85 and 0.80–0.95 for stations north and south of the Alps, respectively, showing that traffic contributes on average only up to 30% to OC. Furthermore, the elevated $f_{NF,OC}$ values together with high correlations with other wood burning markers (non-fossil EC, levoglucosan and water soluble potassium) indicate that residential wood burning is the major source of OC during winter smog episodes in Switzerland. The station-to-station differences and the variability at each individual location north of the Alps is small suggesting that on the one hand the relative source contributions, meteorological conditions, as well as the degree of atmospheric processing and secondary OC formation for the chosen days were very similar and on the other hand that different stations, especially those on the Swiss plateau, are rather influenced by regional air pollution than from local sources. The relative non-fossil contributions of EC ($f_{NF,EC}$), which can be exclusively attributed to wood burning, are on average 0.42 ± 0.13 and 0.49 ± 0.15 for stations north and

south of the Alps, respectively. Since $f_{NF,EC}$ values are often close to 0.5 (even slightly higher for some stations) this shows that also residential wood combustion contributes to a large extent to EC during winter-smog episodes in Switzerland. The sum of non-fossil OC and EC contributes on average 70 ± 18% and 79 ± 10% to total carbon at stations north and south of the Alps, respectively, highlighting the importance of wood burning emissions from residential heating in Switzerland during winter-smog episodes. This is in agreement with recent studies which have shown that residential wood burning can be the dominating source of carbonaceous aerosols during the cold season, in Europe.

The comparison between fossil EC (EC_F, only emitted as primary aerosol) and nitrogen oxides (NO_x), which are mainly associated with traffic emissions, showed a good agreement whereas no correlation was observed between fossil OC (OC_F) and the two latter components, indicating that a considerable amount of OC_F is secondary OC (SOC) formed from fossil precursors mainly emitted from traffic. Correlations between non-fossil OC (OC_{NF}) and EC (EC_{NF}) and the wood burning markers levoglucosan and water soluble potassium (K^+) clearly show different slopes for stations north and south of the Alps suggesting different burning technologies in both regions.

Acknowledgements

This work was funded by the Swiss Federal Office for the Environment (BAFU), inNet Monitoring AG, OSTLUFT, the country Liechtenstein and the Swiss cantons Basel-Stadt, Basel-Landschaft, Graubünden, St.Gallen, Solothurn, Valais, Uri and Ticino.

References

Andersson, A., Sheesley, R. J., Kruså, M., Johansson, C., and Gustafsson, Ö.: 14C-based source assessment of soot aerosols in Stockholm and the Swedish EMEP-Aspvreten regional background site, Atmos. Environ., 45, 215-222, doi: 10.1016/j.atmosenv.2010.09.015, 2011.

BAG - Bundesamt für Gesundheit, Jahresberichte Umweltradioaktivität und Strahlendosen: Umweltradioaktivität und Strahlendosen in der Schweiz 2007, available at: http://www.bag.admin.ch/themen/strahlung/00043/00065/02239/index.html?lang=de (last access: 30 April 2014), 2008.

Barmpadimos, I., Hueglin, C., Keller, J., Henne, S., and Prévôt, A. S. H.: Influence of meteorology on PM10 trends and variability in Switzerland from 1991 to 2008, Atmos. Chem. Phys., 11, 1813-1835, doi: 10.5194/acp-11-1813-2011, 2011.

Bernardoni, V., Calzolai, G., Chiari, M., Fedi, M., Lucarelli, F., Nava, S., Piazzalunga, A., Riccobono, F., Taccetti, F., Valli, G., and Vecchi, R.: Radiocarbon analysis on organic and elemental carbon in aerosol samples and source apportionment at an urban site in Northern Italy, J. Aerosol. Sci., 56, 88-99, doi: 10.1016/j.jaerosci.2012.06.001, 2013.

Canonaco, F., Crippa, M., Slowik, J. G., Baltensperger, U., and Prévôt, A. S. H.: SoFi, an IGOR-based interface for the efficient use of the generalized multilinear engine (ME-2) for the source apportionment: ME-2 application to aerosol mass spectrometer data, Atmos. Meas. Tech., 6, 3649-3661, doi: 10.5194/amt-6-3649-2013, 2013.

Caseiro, A., Bauer, H., Schmidl, C., Pio, C. A., and Puxbaum, H.: Wood burning impact on PM10 in three Austrian regions, Atmos. Environ., 43, 2186-2195, doi: 10.1016/j.atmosenv.2009.01.012, 2009.

Cavalli, F., Viana, M., Yttri, K. E., Genberg, J., and Putaud, J. P.: Toward a standardised thermal-optical protocol for measuring atmospheric organic and elemental carbon: The EUSAAR protocol, Atmos. Meas. Tech., 3, 79-89, doi: 10.5194/amt-3-79-2010, 2010.

Ceburnis, D., Garbaras, A., Szidat, S., Rinaldi, M., Fahrni, S., Perron, N., Wacker, L., Leinert, S., Remeikis, V., Facchini, M. C., Prevot, A. S. H., Jennings, S. G., Ramonet, M., and O'Dowd, C. D.: Quantification of the carbonaceous matter origin in submicron marine aerosol by 13C and 14C isotope analysis, Atmos. Chem. Phys., 11, 8593-8606, doi: 10.5194/acp-11-8593-2011, 2011.

Cercl'Air – Schweizerische Gesellschaft der Lufthygiene-Fachleute: available at: http://www.cerclair.ch/cmsv2/index.php (last access: 30 April 2014), 2012.

Chow, J. C., Watson, J. G., Pritchett, L. C., Pierson, W. R., Frazier, C. A., and Purcell, R. G.: The DRI thermal optical reflectance carbon analysis system - Description, evaluation and application in United-States air-quality studies, Atmos. Environ., Part a - General Topics, 27, 1185-1201, doi: 10.1016/0960-1686(93)90245-t, 1993.

Chow, J. C., Watson, J. G., Crow, D., Lowenthal, D. H., and Merrifield, T.: Comparison of IMPROVE and NIOSH carbon measurements, Aerosol Sci. Technol., 34, 23-34, doi: 10.1080/027868201300081923, 2001.

Dusek, U., Monaco, M., Prokopiou, M., Gongriep, F., Hitzenberger, R., Meijer, H. A. J., and Röckmann, T.: Evaluation of a two-step thermal method for separating organic and elemental carbon for radiocarbon analysis, Atmos. Meas. Tech., 7, 1943-1955, doi: 10.5194/amt-7-1943-2014, 2014.

El Haddad, I., D'Anna, B., Temime-Roussel, B., Nicolas, M., Boreave, A., Favez, O., Voisin, D., Sciare, J., George, C., Jaffrezo, J. L., Wortham, H., and Marchand, N.: Towards a better understanding of the origins, chemical composition and aging of oxygenated organic aerosols: case study of a Mediterranean industrialized environment, Marseille, Atmos. Chem. Phys., 13, 7875-7894, doi: 10.5194/acp-13-7875-2013, 2013.

EMPA: Technischer Bericht zum Nationalen Beobachtungsnetz für Luftfremdstoffe (NABEL), Dübendorf, Switzerland, 2013.

Engling, G., Carrico, C. M., Kreidenweis, S. M., Collett Jr, J. L., Day, D. E., Malm, W. C., Lincoln, E., Min Hao, W., Iinuma, Y., and Herrmann, H.: Determination of levoglucosan in biomass combustion aerosol by high-performance anion-exchange chromatography with pulsed amperometric detection, Atmos. Environ., 40, Supplement 2, 299-311, doi: 10.1016/j.atmosenv.2005.12.069, 2006.

Favez, O., El Haddad, I., Piot, C., Boréave, A., Abidi, E., Marchand, N., Jaffrezo, J. L., Besombes, J. L., Personnaz, M. B., Sciare, J., Wortham, H., George, C., and D'Anna, B.: Inter-comparison of source apportionment models for the estimation of wood burning aerosols during wintertime in an Alpine city (Grenoble, France), Atmos. Chem. Phys., 10, 5295-5314, doi: 10.5194/acp-10-5295-2010, 2010.

833 Gehrig, R., and Buchmann, B.: Characterising seasonal variations and spatial distribution of
834 ambient PM10 and PM2.5 concentrations based on long-term Swiss monitoring data, Atmos.
835 Environ., 37, 2571-2580, doi: 10.1016/s1352-2310(03)00221-8, 2003.

836 Gehrig, R., Hueglin, C., Schwarzenbach, B., Seitz, T., and Buchmann, B.: A new method to
837 link PM10 concentrations from automatic monitors to the manual gravimetric reference
838 method according to EN12341, Atmos. Environ., 39, 2213-2223, doi:
839 10.1016/j.atmosenv.2005.01.005, 2005.

840 Gelencsér, A.: Carbonaceous Aerosols, Springer, Dordrecht, 2004.

841 Gelencsér, A., May, B., Simpson, D., Sánchez-Ochoa, A., Kasper-Giebl, A., Puxbaum, H.,
842 Caseiro, A., Pio, C., and Legrand, M.: Source apportionment of PM2.5 organic aerosol over
843 Europe: Primary/secondary, natural/anthropogenic, and fossil/biogenic origin, J. Geophys.
844 Res.-Atmos., 112, D23S04, doi: 10.1029/2006JD008094, 2007.

845 Genberg, J., Hyder, M., Stenström, K., Bergström, R., Simpson, D., Fors, E. O., Jönsson, J.
846 Å., and Swietlicki, E.: Source apportionment of carbonaceous aerosol in southern Sweden,
847 Atmos. Chem. Phys., 11, 11387-11400, doi: 10.5194/acp-11-11387-2011, 2011.

848 Gianini, M. F. D., Fischer, A., Gehrig, R., Ulrich, A., Wichser, A., Piot, C., Besombes, J. L.,
849 and Hueglin, C.: Comparative source apportionment of PM10 in Switzerland for 2008/2009
850 and 1998/1999 by Positive Matrix Factorisation, Atmos. Environ., 54, 149-158, doi:
851 10.1016/j.atmosenv.2012.02.036, 2012.

852 Gianini, M. F. D., Piot, C., Herich, H., Besombes, J. L., Jaffrezo, J. L., and Hueglin, C.:
853 Source apportionment of PM10, organic carbon and elemental carbon at Swiss sites: An
854 intercomparison of different approaches, Science of The Total Environment, 454–455, 99-
855 108, doi: 10.1016/j.scitotenv.2013.02.043, 2013.

856 Gilardoni, S., Vignati, E., Cavalli, F., Putaud, J. P., Larsen, B. R., Karl, M., Stenstrom, K.,
857 Genberg, J., Henne, S., and Dentener, F.: Better constraints on sources of carbonaceous
858 aerosols using a combined (14C) - Macro tracer analysis in a European rural background site,
859 Atmos. Chem. Phys., 11, 5685-5700, doi: 10.5194/acp-11-5685-2011, 2011.

860 Glasius, M., la Cour, A., and Lohse, C.: Fossil and nonfossil carbon in fine particulate matter:
861 A study of five European cities, J. Geophys. Res., 116, D11302, doi: 10.1029/2011JD015646
862 2011.

Hallquist, M., Wenger, J. C., Baltensperger, U., Rudich, Y., Simpson, D., Claeys, M., Dommen, J., Donahue, N. M., George, C., Goldstein, A. H., Hamilton, J. F., Herrmann, H., Hoffmann, T., Iinuma, Y., Jang, M., Jenkin, M. E., Jimenez, J. L., Kiendler-Scharr, A., Maenhaut, W., McFiggans, G., Mentel, T. F., Monod, A., Prévôt, A. S. H., Seinfeld, J. H., Surratt, J. D., Szmigielski, R., and Wildt, J.: The formation, properties and impact of secondary organic aerosol: Current and emerging issues, Atmos. Chem. Phys., 9, 5155-5236, doi: 10.5194/acp-9-5155-2009, 2009.

Harrison, R. M., Beddows, D. C. S., Hu, L., and Yin, J.: Comparison of methods for evaluation of wood smoke and estimation of UK ambient concentrations, Atmos. Chem. Phys., 12, 8271-8283, doi: 10.5194/acp-12-8271-2012, 2012.

Heal, M. R.: The application of carbon-14 analyses to the source apportionment of atmospheric carbonaceous particulate matter: a review, Analytical and Bioanalytical Chemistry, 406, 81-98, doi: 10.1007/s00216-013-7404-1, 2014.

Hennigan, C. J., Miracolo, M. A., Engelhart, G. J., May, A. A., Presto, A. A., Lee, T., Sullivan, A. P., McMeeking, G. R., Coe, H., Wold, C. E., Hao, W. M., Gilman, J. B., Kuster, W. C., de Gouw, J., Schichtel, B. A., J. L. Collett, J., Kreidenweis, S. M., and Robinson, A. L.: Chemical and physical transformations of organic aerosol from the photo-oxidation of open biomass burning emissions in an environmental chamber, Atmos. Chem. Phys., 11, 7669-7686, doi: 10.5194/acp-11-7669-2011, 2011.

Herich, H., Hueglin, C., and Buchmann, B.: A 2.5 year's source apportionment study of black carbon from wood burning and fossil fuel combustion at urban and rural sites in Switzerland, Atmos. Meas. Tech., 4, 1409-1420, doi: 10.5194/amt-4-1409-2011, 2011.

Herich, H., Gianini, M. F. D., Piot, C., Močnik, G., Jaffrezo, J. L., Besombes, J. L., Prévôt, A. S. H., and Hueglin, C.: Overview of the impact of wood burning emissions on carbonaceous aerosols and PM in large parts of the Alpine region, Atmos. Environ., 89, 64-75, doi: 10.1016/j.atmosenv.2014.02.008, 2014.

Heringa, M. F., DeCarlo, P. F., Chirico, R., Tritscher, T., Dommen, J., Weingartner, E., Richter, R., Wehrle, G., Prevot, A. S. H., and Baltensperger, U.: Investigations of primary and secondary particulate matter of different wood combustion appliances with a high-resolution time-of-flight aerosol mass spectrometer, Atmos. Chem. Phys., 11, 5945-5957, doi: 10.5194/acp-11-5945-2011, 2011.

Hodzic, A., Jimenez, J. L., Prévôt, A. S. H., Szidat, S., Fast, J. D., and Madronich, S.: Can 3-D models explain the observed fractions of fossil and non-fossil carbon in and near Mexico City?, Atmos. Chem. Phys., 10, 10997-11016, doi: 10.5194/acp-10-10997-2010, 2010.

Huang, J., Kang, S., Shen, C., Cong, Z., Liu, K., Wang, W., and Liu, L.: Seasonal variations and sources of ambient fossil and biogenic-derived carbonaceous aerosols based on 14C measurements in Lhasa, Tibet, Atmospheric Research, 96, 553-559, doi: 10.1016/j.atmosres.2010.01.003, 2010.

IPCC: Climate Change 2013: the physical science basis. Contribution of working group I to the fifth Assessment Report of the Intergovernmental Panel on Climate Change [Stocker, T.F., D. Qin, G.-K. Plattner, M. Tignor, S.K. Allen, J. Boschung, A. Nauels, Y. Xia, V. Bex and P.M. Midgley (eds.)], Cambridge University Press, Cambridge, United Kingdom and New York, NY, USA, 2013.

Jacobson, M. C., Hansson, H. C., Noone, K. J., and Charlson, R. J.: Organic atmospheric aerosols: Review and state of the science, Rev. Geophys., 38, 267-294, doi: 10.1029/1998RG000045, 2000.

Jimenez, J. L., Canagaratna, M. R., Donahue, N. M., Prevot, A. S. H., Zhang, Q., Kroll, J. H., DeCarlo, P. F., Allan, J. D., Coe, H., Ng, N. L., Aiken, A. C., Docherty, K. S., Ulbrich, I. M., Grieshop, A. P., Robinson, A. L., Duplissy, J., Smith, J. D., Wilson, K. R., Lanz, V. A., Hueglin, C., Sun, Y. L., Tian, J., Laaksonen, A., Raatikainen, T., Rautiainen, J., Vaattovaara, P., Ehn, M., Kulmala, M., Tomlinson, J. M., Collins, D. R., Cubison, M. J., E, Dunlea, J., Huffman, J. A., Onasch, T. B., Alfarra, M. R., Williams, P. I., Bower, K., Kondo, Y., Schneider, J., Drewnick, F., Borrmann, S., Weimer, S., Demerjian, K., Salcedo, D., Cottrell, L., Griffin, R., Takami, A., Miyoshi, T., Hatakeyama, S., Shimono, A., Sun, J. Y., Zhang, Y. M., Dzepina, K., Kimmel, J. R., Sueper, D., Jayne, J. T., Herndon, S. C., Trimborn, A. M., Williams, L. R., Wood, E. C., Middlebrook, A. M., Kolb, C. E., Baltensperger, U., and Worsnop, D. R.: Evolution of organic aerosols in the atmosphere, Science, 326, 1525-1529, doi: 10.1126/science.1180353, 2009.

Johansson, L. S., Tullin, C., Leckner, B., and Sjövall, P.: Particle emissions from biomass combustion in small combustors, Biomass and Bioenergy, 25, 435-446, doi: 10.1016/S0961-9534(03)00036-9, 2003.

924 Kessler, S. H., Smith, J. D., Che, D. L., Worsnop, D. R., Wilson, K. R., and Kroll, J. H.:
925 Chemical sinks of organic aerosol: Kinetics and products of the heterogeneous oxidation of
926 erythritol and levoglucosan, Environ. Sci. Technol., 44, 7005-7010, doi: 10.1021/es101465m,
927 2010.

928 Khalil, M. A. K., and Rasmussen, R. A.: Tracers of wood smoke, Atmos. Environ., 37, 1211-
929 1222, doi: 10.1016/S1352-2310(02)01014-2, 2003.

930 Lanz, V. A., Alfarra, M. R., Baltensperger, U., Buchmann, B., Hueglin, C., Szidat, S., Wehrli,
931 M. N., Wacker, L., Weimer, S., Caseiro, A., Puxbaum, H., and Prevot, A. S. H.: Source
932 attribution of submicron organic aerosols during wintertime inversions by advanced factor
933 analysis of aerosol mass spectra, Environ. Sci. Technol., 42, 214-220, doi:
934 10.1021/es0707207, 2008.

935 Lanz, V. A., Prévôt, A. S. H., Alfarra, M. R., Weimer, S., Mohr, C., DeCarlo, P. F., Gianini,
936 M. F. D., Hueglin, C., Schneider, J., Favez, O., D'Anna, B., George, C., and Baltensperger,
937 U.: Characterization of aerosol chemical composition with aerosol mass spectrometry in
938 Central Europe: An overview, Atmos. Chem. Phys., 10, 10453-10471, doi: 10.5194/acp-10-
939 10453-2010, 2010.

940 Larsen, B. R., Gilardoni, S., Stenström, K., Niedzialek, J., Jimenez, J., and Belis, C. A.:
941 Sources for PM air pollution in the Po Plain, Italy: II. Probabilistic uncertainty
942 characterization and sensitivity analysis of secondary and primary sources, Atmos. Environ.,
943 50, 203-213, doi: 10.1016/j.atmosenv.2011.12.038, 2012.

944 Lee, T., Sullivan, A. P., Mack, L., Jimenez, J. L., Kreidenweis, S. M., Onasch, T. B.,
945 Worsnop, D. R., Malm, W., Wold, C. E., Hao, W. M., and Collett, J. L.: Chemical smoke
946 marker emissions during flaming and smoldering phases of laboratory open burning of
947 wildland fuels, Aerosol Sci. Technol., 44, I-V, doi: 10.1080/02786826.2010.499884, 2010.

948 Levin, I., Naegler, T., Kromer, B., Diehl, M., Francey, R. J., Gomez-Pelaez, A. J., Steele, L.
949 P., Wagenbach, D., Weller, R., and Worthy, D. E.: Observations and modelling of the global
950 distribution and long-term trend of atmospheric $^{14}CO_2$, Tellus B, 62, 26-46, doi:
951 10.1111/j.1600-0889.2009.00446.x, 2010.

952 Liu, D., Allan, J. D., Young, D. E., Coe, H., Beddows, D., Fleming, Z. L., Flynn, M. J.,
953 Gallagher, M. W., Harrison, R. M., Lee, J., Prevot, A. S. H., Taylor, J. W., Yin, J., Williams,
954 P. I., and Zotter, P.: Size distribution, mixing state and source apportionments of black carbon

aerosols in London during winter time, Atmos. Chem. Phys. Discuss., 14, 16291-16349, doi: 10.5194/acpd-14-16291-2014, 2014.

Federal Office of Meteorology and Climatology (MeteoSwiss): available at: http://www.meteoschweiz.admin.ch/web/en.html (last access: 30 April 2014), 2014.

Minguillón, M. C., Perron, N., Querol, X., Szidat, S., Fahrni, S. M., Alastuey, A., Jimenez, J. L., Mohr, C., Ortega, A. M., Day, D. A., Lanz, V. A., Wacker, L., Reche, C., Cusack, M., Amato, F., Kiss, G., Hoffer, A., Decesari, S., Moretti, F., Hillamo, R., Teinilä, K., Seco, R., Peñuelas, J., Metzger, A., Schallhart, S., Müller, M., Hansel, A., Burkhart, J. F., Baltensperger, U., and Prévôt, A. S. H.: Fossil versus contemporary sources of fine elemental and organic carbonaceous particulate matter during the DAURE campaign in Northeast Spain, Atmos. Chem. Phys., 11, 12067-12084, doi: 10.5194/acp-11-12067-2011, 2011.

Mohn, J., Szidat, S., Fellner, J., Rechberger, H., Quartier, R., Buchmann, B., and Emmenegger, L.: Determination of biogenic and fossil CO_2 emitted by waste incineration based on (CO_2)-C-14 and mass balances, Bioresource Technol., 99, 6471-6479, doi: 10.1016/j.biortech.2007.11.042, 2008.

NIOSH: Elemental Carbon (Diesel Particulate): Method 5040, www.cdc.gov./niosh/nmam/pdfs/5040f3.pdf (last access: 30 April 2014), 1999.

Swiss Federal Statistical Office: Forstwirtschaft , available at: http://www.bfs.admin.ch/bfs/portal/de/index/themen/07/04.html (last access: 30 April 2014), 2014.

Perron, N., Sandradewi, J., Alfarra, M. R., Lienemann, P., Gehrig, R., Kasper-Giebl, A., Lanz, V. A., Szidat, S., Ruff, M., Fahrni, S., Wacker, L., Baltensperger, U., and Prévôt, A. S. H.: Composition and sources of particulate matter in an industrialised Alpine valley, Atmos. Chem. Phys. Discuss., 10, 9391-9430, doi: 10.5194/acpd-10-9391-2010, 2010.

Peterson, M. R., and Richards, M. H.: Thermal-optical transmittance analysis for organic, elemental, carbonate, total carbon, and OCX2 in PM2.5 by the EPA/NIOSH method, in: Proceedings, Symposium on Air Quality Measurement Methods and Technology-2002, edited by: Winegar, E. D. and Tropp, R. J., Air & Waste Management Association, Pittsburgh, PA, 83-1-83-19, 2002.

Piazzalunga, A., Fermo, P., Bernardoni, V., Vecchi, R., Valli, G., and De Gregorio, M. A.: A simplified method for levoglucosan quantification in wintertime atmospheric particulate

matter by high performance anion-exchange chromatography coupled with pulsed amperometric detection, Int. J. Environ. Anal. Chem., 90, 934-947, doi: 10.1080/03067310903023619, 2010.

Piazzalunga, A., Bernardoni, V., Fermo, P., Valli, G., and Vecchi, R.: Technical Note: On the effect of water-soluble compounds removal on EC quantification by TOT analysis in urban aerosol samples, Atmos. Chem. Phys., 11, 10193-10203, doi: 10.5194/acp-11-10193-2011, 2011a.

Piazzalunga, A., Belis, C., Bernardoni, V., Cazzuli, O., Fermo, P., Valli, G., and Vecchi, R.: Estimates of wood burning contribution to PM by the macro-tracer method using tailored emission factors, Atmos. Environ., 45, 6642-6649, doi: 10.1016/j.atmosenv.2011.09.008, 2011b.

Piazzalunga, A., Bernardoni, V., Fermo, P., and Vecchi, R.: Optimisation of analytical procedures for the quantification of ionic and carbonaceous fractions in the atmospheric aerosol and applications to ambient samples, Analytical and Bioanalytical Chemistry, 405, 1123-1132, doi: 10.1007/s00216-012-6433-5, 2013a.

Piazzalunga, A., Anzano, M., Collina, E., Lasagni, M., Lollobrigida, F., Pannocchia, A., Fermo, P., and Pitea, D.: Contribution of wood combustion to PAH and PCDD/F concentrations in two urban sites in Northern Italy, J. Aerosol. Sci., 56, 30-40, doi: 10.1016/j.jaerosci.2012.07.005, 2013b.

Pope, C. A., and Dockery, D. W.: Health effects of fine particulate air pollution: Lines that connect, J. Air Waste Manage. Assoc., 56, 709-742, doi: 10.1080/10473289.2006.10464485, 2006.

Pöschl, U.: Atmospheric aerosols: Composition, transformation, climate and health effects, Angew. Chem. Int. Edt., 44, 7520-7540, doi: 10.1002/anie.200501122, 2005.

Putaud, J.-P., Raes, F., Van Dingenen, R., Brüggemann, E., Facchini, M. C., Decesari, S., Fuzzi, S., Gehrig, R., Hüglin, C., Laj, P., Lorbeer, G., Maenhaut, W., Mihalopoulos, N., Müller, K., Querol, X., Rodriguez, S., Schneider, J., Spindler, G., Brink, H. t., Tørseth, K., and Wiedensohler, A.: A European aerosol phenomenology-2: chemical characteristics of particulate matter at kerbside, urban, rural and background sites in Europe, Atmos. Environ., 38, 2579-2595, doi: 10.1016/j.atmosenv.2004.01.041, 2004.

Ruff, M., Wacker, L., Gaggeler, H. W., Suter, M., Synal, H. A., and Szidat, S.: A gas ion source for radiocarbon measurements at 200 kV, Radiocarbon, 49, 307-314, doi, 2007.

Ruff, M., Szidat, S., Gäggeler, H. W., Suter, M., Synal, H. A., and Wacker, L.: Gaseous radiocarbon measurements of small samples, Nucl. Instr. Methods Phys. Res., Sec. B, 268, 790-794, doi: 10.1016/j.nimb.2009.10.032, 2010.

Ruffieux, D., Nash, J., Jeannet, P., and Agnew, J. L.: The COST 720 temperature, humidity, and cloud profiling campaign: TUC, Meteorol. Z., 15, 5-10, doi: 10.1127/0941-2948/2006/0095, 2006.

Sandradewi, J., Prevot, A. S. H., Szidat, S., Perron, N., Alfarra, M. R., Lanz, V. A., Weingartner, E., and Baltensperger, U.: Using aerosol light absorption measurements for the quantitative determination of wood burning and traffic emission contributions to particulate matter, Environ. Sci. Technol., 42, 3316-3323, doi: 10.1021/es702253m, 2008a.

Sandradewi, J., Prévôt, A. S. H., Alfarra, M. R., Szidat, S., Wehrli, M. N., Ruff, M., Weimer, S., Lanz, V. A., Weingartner, E., Perron, N., Caseiro, A., Kasper-Giebl, A., Puxbaum, H., Wacker, L., and Baltensperger, U.: Comparison of several wood smoke markers and source apportionment methods for wood burning particulate mass, Atmos. Chem. Phys. Discuss., 8, 8091-8118, doi: 10.5194/acpd-8-8091-2008, 2008b.

Schauer, J. J., Kleeman, M. J., Cass, G. R., and Simoneit, B. R. T.: Measurement of emissions from air pollution sources. 1. C1 through C29 organic compounds from meat charbroiling, Environ. Sci. Technol., 33, 1566-1577, doi: 10.1021/es980076j, 1999.

Schauer, J. J., Kleeman, M. J., Cass, G. R., and Simoneit, B. R. T.: Measurement of emissions from air pollution sources. 3. C1−C29 organic compounds from fireplace combustion of wood, Environ. Sci. Technol., 35, 1716-1728, doi: 10.1021/es001331e, 2001.

Schmid, H., Laskus, L., Abraham, H. J., Baltensperger, U., Lavanchy, V., Bizjak, M., Burba, P., Cachier, H., Crow, D., Chow, J., Gnauk, T., Even, A., ten Brink, H. M., Giesen, K.-P., Hitzenberger, R., Hueglin, C., Maenhaut, W., Pio, C., Carvalho, A., Putaud, J.-P., Toom-Sauntry, D., and Puxbaum, H.: Results of the "carbon conference" international aerosol carbon round robin test stage I, Atmos. Environ., 35, 2111-2121, doi, 2001.

Schmidl, C., Marr, I. L., Caseiro, A., Kotianová, P., Berner, A., Bauer, H., Kasper-Giebl, A., and Puxbaum, H.: Chemical characterisation of fine particle emissions from wood stove

combustion of common woods growing in mid-European Alpine regions, Atmos. Environ., 42, 126-141, doi: 10.1016/j.atmosenv.2007.09.028, 2008.

Schmidl, C., Luisser, M., Padouvas, E., Lasselsberger, L., Rzaca, M., Ramirez-Santa Cruz, C., Handler, M., Peng, G., Bauer, H., and Puxbaum, H.: Particulate and gaseous emissions from manually and automatically fired small scale combustion systems, Atmos. Environ., 45, 7443-7454, doi: 10.1016/j.atmosenv.2011.05.006, 2011.

Steinbacher, M., Zellweger, C., Schwarzenbach, B., Bugmann, S., Buchmann, B., Ordóñez, C., Prevot, A. S. H., and Hueglin, C.: Nitrogen oxide measurements at rural sites in Switzerland: Bias of conventional measurement techniques, J. Geophys. Res.-Atmos., 112, D11307, doi: 10.1029/2006JD007971, 2007.

Stuiver, M., and Polach, H. A.: Reporting of C-14 data - discussion, Radiocarbon, 19, 355-363, doi, 1977.

Synal, H. A., Stocker, M., and Suter, M.: MICADAS: A new compact radiocarbon AMS system, Nucl. Instr. Methods Phys. Res., Sec. B, 259, 7-13, doi: 10.1016/j.nimb.2007.01.138, 2007.

Szidat, S., Jenk, T. M., Gäggeler, H. W., Synal, H. A., Fisseha, R., Baltensperger, U., Kalberer, M., Samburova, V., Wacker, L., Saurer, M., Schwikowski, M., and Hajdas, I.: Source apportionment of aerosols by 14C measurements in different carbonaceous particle fractions, Radiocarbon, 46, 475-484, doi, 2004.

Szidat, S., Jenk, T. M., Synal, H. A., Kalberer, M., Wacker, L., Hajdas, I., Kasper-Giebl, A., and Baltensperger, U.: Contributions of fossil fuel, biomass-burning, and biogenic emissions to carbonaceous aerosols in Zurich as traced by 14C, J. Geophys. Res.-Atmos., 111, doi: 10.1029/2005JD006590, 2006.

Szidat, S., Prévôt, A. S. H., Sandradewi, J., Alfarra, M. R., Synal, H.-A., Wacker, L., and Baltensperger, U.: Dominant impact of residential wood burning on particulate matter in Alpine valleys during winter, Geophys. Res. Lett., 34, L05820, doi: 10.1029/2006GL028325, 2007.

Szidat, S.: Sources of Asian haze, Science, 323, 470-471, doi: 10.1126/science.1169407, 2009.

1075 Szidat, S., Ruff, M., Perron, N., Wacker, L., Synal, H. A., Hallquist, M., Shannigrahi, A. S.,
1076 Yttri, K. E., Dye, C., and Simpson, D.: Fossil and non-fossil sources of organic carbon (OC)
1077 and elemental carbon (EC) in Göteborg, Sweden, Atmos. Chem. Phys., 9, 1521-1535, doi:
1078 10.5194/acp-9-1805-2009, 2009.

1079 Szidat, S., Bench, G., Bernardoni, V., Calzolai, G., Czimczik, C. I., Derendorp, L., Dusek, U.,
1080 Elder, K., Fedi, M. E., Genberg, J., Gustafsson, O., Kirillova, E., Kondo, M., McNichol, A.
1081 P., Perron, N., Santos, G. M., Stenstrom, K., Swietlicki, E., Uchida, M., Vecchi, R., Wacker,
1082 L., Zhang, Y. L., and Prevot, A. S. H.: Intercomparison of C-14 analysis of carbonaceous
1083 aerosols: exercise 2009, Radiocarbon, 56, 561-566, doi: 10.2458/azu_js_rc.55.16314, 2013.

1084 Szidat, S., Salazar, G. A., Vogel, E., Battaglia, M., Wacker, L., Synal, H.-A., and Türler, A.:
1085 14C analysis and sample preparation at the new Bern Laboratory for the Analysis of
1086 Radiocarbon with AMS (LARA), Radiocarbon, doi: 10.2458/56.17457, 2014.

1087 Tanner, R. L., Parkhurst, W. J., and McNichol, A. P.: Fossil sources of ambient aerosol
1088 carbon based on 14C measurements, Aerosol Sci. Technol., 38, 133 - 139, doi, 2004.

1089 Turpin, B. J., and Lim, H. J.: Species contributions to PM2.5 mass concentrations: Revisiting
1090 common assumptions for estimating organic mass, Aerosol Sci. Technol., 35, 602-610, doi:
1091 10.1080/02786820152051454, 2001.

1092 Valmari, T., Kauppinen, E. I., Kurkela, J., Jokiniemi, J. K., Sfiris, G., and Revitzer, H.: Fly
1093 ash formation and deposition during fluidized bed combustion of willow, J. Aerosol. Sci., 29,
1094 445-459, doi: 10.1016/S0021-8502(97)10021-0, 1998.

1095 Viana, M., Chi, X., Maenhaut, W., Cafmeyer, J., Querol, X., Alastuey, A., Mikuška, P., and
1096 Večeřa, Z.: Influence of sampling artefacts on measured PM, OC, and EC levels in
1097 carbonaceous aerosols in an urban area, Aerosol Sci. Technol., 40, 107-117, doi:
1098 10.1080/02786820500484388, 2006.

1099 Viana, M., Maenhaut, W., ten Brink, H. M., Chi, X., Weijers, E., Querol, X., Alastuey, A.,
1100 Mikuška, P., and Večeřa, Z.: Comparative analysis of organic and elemental carbon
1101 concentrations in carbonaceous aerosols in three European cities, Atmos. Environ., 41, 5972-
1102 5983, doi: 10.1016/j.atmosenv.2007.03.035, 2007.

1103 Wacker, L., Christl, M., and Synal, H. A.: Bats: A new tool for AMS data reduction, Nucl.
1104 Instr. Methods Phys. Res., Sec. B, 268, 976-979, doi: 10.1016/j.nimb.2009.10.078, 2010.

Wacker, L., Fahrni, S. M., Hajdas, I., Molnar, M., Synal, H. A., Szidat, S., and Zhang, Y. L.: A versatile gas interface for routine radiocarbon analysis with a gas ion source, Nucl. Instr. Methods Phys. Res., Sec. B, 294, 315-319, doi: 10.1016/j.nimb.2012.02.009, 2013.

WHO: Air Quality Guidelines for Particulate Matter, Ozone, Nitrogen Dioxide and Sulfur Dioxide, Global Update 2005, Summary of Risk Assessment, World Health Organization, document WHO/SDE/PHE/OEH/06.02, Geneva, 2006.

Zapf, A., Nesje, A., Szidat, S., Wacker, L., and Schwikowski, M.: C-14 measurements of ice samples from the Juvfonne ice tunnel, Jotunheimen, southern Norway-validation of a C-14 dating technique for glacier ice, Radiocarbon, 55, 571-578, doi: doi:10.2458/azu_js_rc.55.16320, 2013.

Zencak, Z., Elmquist, M., and Gustafsson, O.: Quantification and radiocarbon source apportionment of black carbon in atmospheric aerosols using the CTO-375 method, Atmos. Environ., 41, 7895-7906, doi: 10.1016/j.atmosenv.2007.06.006, 2007.

Zhang, Y. L., Perron, N., Ciobanu, V. G., Zotter, P., Minguillón, M. C., Wacker, L., Prévôt, A. S. H., Baltensperger, U., and Szidat, S.: On the isolation of OC and EC and the optimal strategy of radiocarbon-based source apportionment of carbonaceous aerosols, Atmos. Chem. Phys., 12, 10841-10856, doi: 10.5194/acp-12-10841-2012, 2012.

Zhang, Y. L., Li, J., Zhang, G., Zotter, P., Huang, R. J., Tang, J. H., Wacker, L., Prevot, A. S., and Szidat, S.: Radiocarbon-based source apportionment of carbonaceous aerosols at a regional background site on hainan island, South China, Environ. Sci. Technol., 48, 2651-2659, doi: 10.1021/es4050852, 2014.

Zotter, P., Zhang, Y. L., El-Haddad, I., Ciobanu, V. G., Daellenbach, K. R., Salazar, G. A., Wacker, L., Herich, H., Hueglin, C., Baltensperger, U., Szidat, S., and Prévôt, A. H. S.: Radiocarbon analysis of elemental and organic carbon in Switzerland during winter-smog episodes from 2008 to 2012 – Part II: Daily, seasonal and yearly variability, in preparation for Atmos. Chem. Phys., 2014.

Table 1: List of all stations, their classification according to the Swiss Federal Office for the Environment (BAFU), their general location in Switzerland, their abbreviations which are used later in the text, figures and tables, as well the different winter seasons from which filters from each station were analyzed.

Station name	Station code	General location	Station type	Altitude	Winter analyzed*
Reiden-A2	REI	north of the Alps/ Swiss Plateau	rural/highway	510m	07/08
Basel-St. Johann	BAS		urban/background	308m	07/08-08/09
Sissach-West	SIS		suburban/traffic	410m	07/08-11/12
Solothurn-Altwyberhüsli	SOL		urban/background	502m	07/08-11/12
Payerne	PAY		rural/background	539m	07/08-11/12
Zürich-Kaserne	ZUR		urban/background	457m	07/08-11/12#
St.Gallen-Rorschacherstrasse	STG		urban/traffic	457m	07/08-11/12
Bern-Bollwerk	BER		urban/traffic	506m	08/09-12/13
Vaduz-Austrasse	VAD	north of the Alps/ alpine valley	suburban/traffic	706m	07/08-11/12
Massongex	MAS		rural/industry	452m	08/09-11/12
Schächental	SCH		rural/background	995m	10/11
Chiasso	CHI	south of the Alps	urban/traffic	291m	07/08-11/12
Magadino-Cadenazzo	MAG		rural/background	254m	07/08-11/12
Moleno-A2	MOL	south of the Alps/ alpine valley	rural/highway	305m	07/08
Roveredo-Stazione	ROV		suburban/background	370m	07/08
San-Vittore	SVI		rural/traffic	330m	07/08-11/12

*EC and OC concentrations, ^{14}C in OC and EC were analyzed on all filters. Levoglucosan was only analyzed for all stations for the winters 2007/2008 and 2008/2009.

#In addition, a yearly cycle from August 2008 to July 2009 with 2-3 samples per month was analyzed for ZUR.

1141 Table 2: Summary of the different correction steps of the ^{14}C raw data.

Correction	**Abbreviations**	
1) <u>blank correction</u> $f_{M,corr} = \frac{mC_{sample} \cdot f_{M,sample} - mC_{blk} \cdot f_{M,blk}}{mC_{sample} - mC_{blk}}$	f_M	fraction of modern from ^{14}C analysis
	$f_{M,sample}$	f_M obtained on the selected filters
	$f_{M,blk}$	f_M obtained on the blank filters
	$f_{M,corr}$	blank corrected f_M
	mC_{sample}	carbon mass of the samples
	mC_{blk}	carbon mass of the blanks
2) <u>EC yield correction</u> $f_{M,EC,total} = slope \cdot (1 - EC_{yield}) + f_{M,EC}$	$f_{M,EC}$	f_M for EC
	EC_{yield}	EC fraction separated for ^{14}C analysis
	slope	slope between $f_{M,EC}$ and EC_{yield} (see Fig. S2)
	$f_{M,EC,total}$	$f_{M,EC}$ corrected to 100% EC_{yield}
3) <u>charring correction</u> $f_{M,EC,final} = \frac{f_{M,EC,total} - f_{M,charr} \cdot f_{charr}}{1 - mC_{charr}}$	$f_{M,charr}$	f_M of charred *OC*
	f_{charr}	fraction of charred OC
	$f_{M,EC,final}$	charring corrected $f_{M,EC,total}$
4) <u>bomb peak correction</u> $f_{NF,ref} = p_{bio} \cdot f_{M,bio} + (1 - p_{bio}) \cdot f_{M,bb}$ $f_{NF,OC} = f_{M,OC,corr} / f_{NF,ref}$ $f_{NF,EC} = f_{M,EC,final} / f_{M,bb}$	p_{bio}	biogenic fraction of total non-fossil sources
	$f_{M,bio}$	f_M of biogenic sources
	$f_{M,bb}$	f_M of biomass burning
	$f_{NF,ref}$	modern ^{14}C content during sampling compared to 1950 (before bomb testing)
	$f_{NF,OC}$	final non-fossil fraction of OC
	$f_{NF,EC}$	final non-fossil fraction of EC

1142

1143

1144

1145

1146

1147

1148

1149

Table 3: Compilation of the ratios between levoglucosan (Levo) and K^+, EC_{NF} and levoglucosan, OC_{NF} and levoglucosan as well as OC_{NF} and EC_{NF} for all stations. Numbers indicate the mean values ± standard deviation. The number of samples is reported in brackets. OC_F values from BAS and all data from the yearly cycle in ZUR are excluded (see Sect. 3.2.1 and Sect. 1). No levoglucosan was measured in SCH. In addition, ratios previously reported in literature* for similar conditions are included as well.

station	EC_{NF}/Levo	OC_{NF}**/Levo	OC_{NF}**/EC_{NF}	Levo/K^+
REI	1.76 ± 0.49 (n = 5)	17.3 ± 4.2 (n = 5)	9.9 ± 1.3 (n = 5)	0.59 ± 0.16 (n = 5)
BER	1.74 ± 0.21 (n = 5)	15.5 ± 2.2 (n = 5)	9.4 ± 1.6 (n = 25)	0.87 ± 0.12 (n = 5)
BAS	1.29 ± 0.28 (n = 9)	-	-	1.52 ± 0.47 (n = 10)
PAY	1.26 ± 0.21 (n = 5)	10.4 ± 1.1 (n = 5)	8.3 ± 2.5 (n = 25)	1.37 ± 0.32 (n = 5)
SIS	1.79 ± 0.46 (n = 9)	12.9 ± 3.7 (n = 8)	6.7 ± 1.4 (n = 21)	0.63 ± 0.21 (n = 10)
SOL	1.42 ± 0.33 (n = 9)	11.8 ± 2.2 (n = 10)	7.8 ± 2.0 (n = 25)	1.05 ± 0.25 (n = 10)
MAS	1.15 ± 0.13 (n = 5)	10.9 ± 2.0 (n = 5)	8.4 ± 1.5 (n = 20)	2.05 ± 0.43 (n = 5)
ZUR	2.12 ± 0.79 (n = 9)	13.1 ± 2.2 (n = 9)	7.3 ± 2.0 (n = 25)	0.80 ± 0.22 (n = 10)
VAD	2.43 ± 0.78 (n = 9)	12.1 ± 3.5 (n = 10)	5.9 ± 1.5 (n = 25)	0.88 ± 0.24 (n = 10)
STG	1.77 ± 0.29 (n = 14)	11.7 ± 2.0 (n = 14)	7.4 ± 1.9 (n = 25)	0.97 ± 0.26 (n = 13)
SCH	-	-	5.1 ± 1.2 (n = 3)	-
MOL	0.77 ± 0.24 (n = 5)	7.3 ± 2.0 (n = 5)	9.9 ± 2.9 (n = 5)	3.67 ± 0.83 (n = 5)
ROV	0.76 ± 0.43 (n = 5)	7.0 ± 3.0 (n = 5)	9.7 ± 2.1 (n = 5)	4.39 ± 1.53 (n = 5)
CHI	1.01 ± 0.28 (n = 10)	9.9 ± 2.8 (n = 10)	9.8 ± 3.7 (n = 25)	2.87 ± 0.97 (n = 10)
MAG	0.80 ± 0.17 (n = 10)	6.9 ± 2.6 (n = 10)	7.9 ± 2.4 (n = 25)	3.29 ± 0.73 (n = 10)
SVI	0.93 ± 0.19 (n = 6)	6.9 ± 1.4 (n = 6)	7.3 ± 1.9 (n = 22)	4.49 ± 1.20 (n = 6)
north of Alps	1.72 ± 0.59 (n = 79)	12.6 ± 3.1 (n = 71)	7.7 ± 2.1 (n = 199)	1.03 ± 0.46 (n = 83)
south of Alps	0.87 ± 0.27 (n = 36)	7.8 ± 2.7 (n = 36)	8.6 ± 2.9 (n = 82)	3.58 ± 1.16 (n = 36)
Austria***	1.31 ± 0.11	7.24 ± 0.03	5.57 ± 0.48	-
Po-valley****	0.89 ± 0.06	5.62 ± 0.30	6.54 ± 0.25	-
north of Alps#	1.82 ± 0.44	9.05 ± 1.77	4.98 ± 0.39	-

south of Alps[‡]	1.20 ± 0.37	7.04 ± 0.90	4.72 ± 0.04	-

[*]data from the publications listed below were summarized and recalculated by Herich et al. (2014)

[**]Herich et al. (2014) obtained biomass burning OC (OC_{BB}) ratios which do not include SOA

[***]average over measurements in winter from Vienna, Graz and Salzburg (Caseiro et al., 2009)

[****]average over measurements in winter from Milan, Sondrio and Ispra (Gilardoni et al., 2011; Piazzalunga et al., 2011b)

[#]average over measurements in winter from BER, PAY, STG, ZUR, REI, BAS, Ebnat-Kappel (Sandradewi et al., 2008b; Herich et al., 2011; Gianini et al., 2012)

[‡]average over measurements in winter from MAG, MOL, ROV (Sandradewi et al., 2008b; Herich et al., 2011; Gianini et al., 2012)

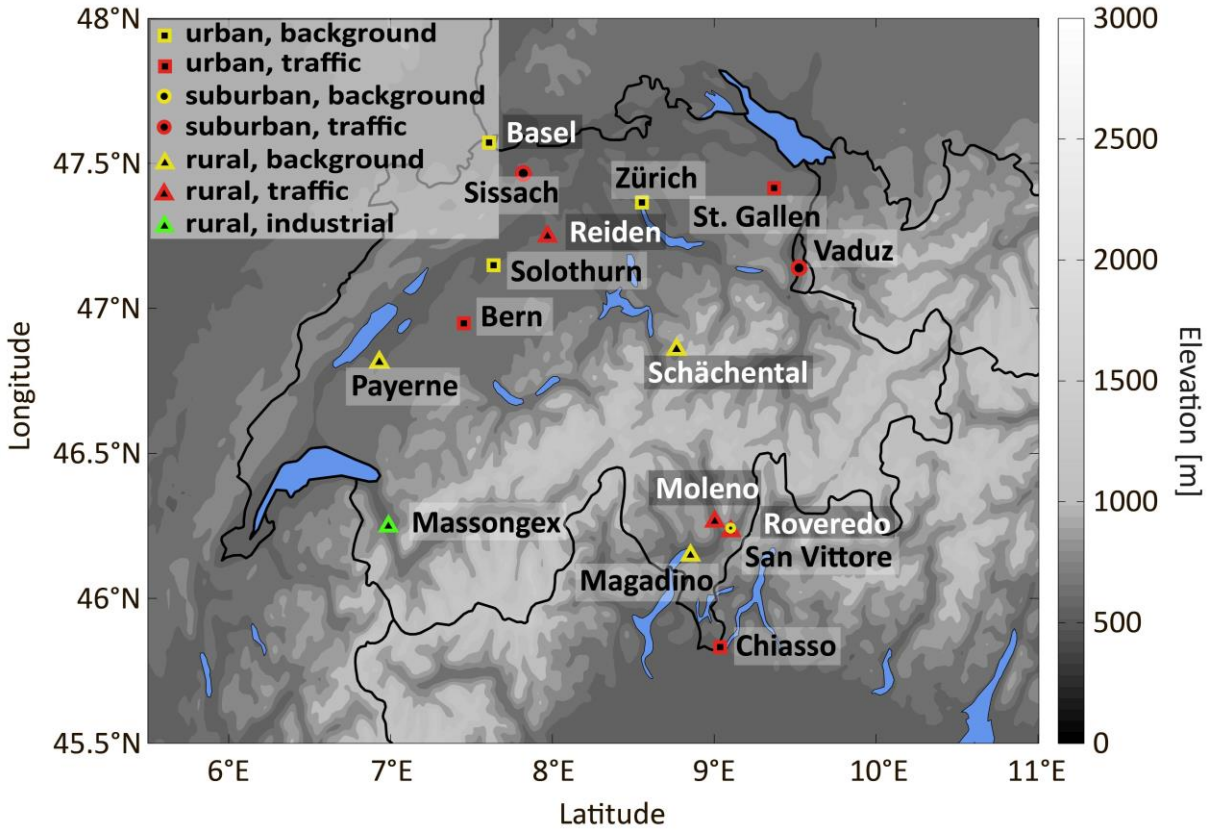

Figure 1: Location of the different stations in Switzerland investigated in this study. White labels indicate stations from which filters from only 1 or 2 winters were analyzed. For all other stations samples from 4 or 5 winters were studied.

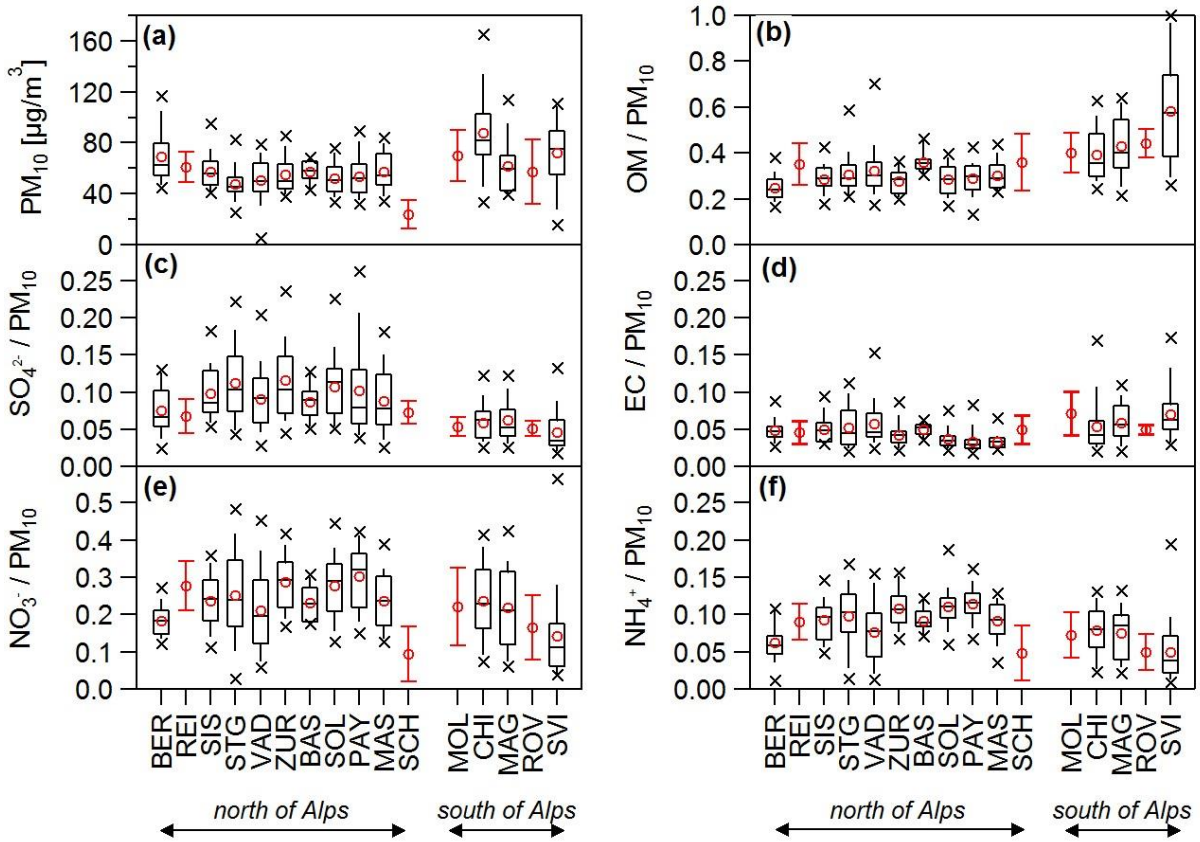

Figure 2: Whisker box plots of the fractional contributions of the major constituents of PM_{10} (water-soluble ions NO_3^-, SO_4^{2-} and NH_4^+ as well as EC and OM = OC * 1.8) from all analyzed winter samples (n ~ 300). The open red circles represent the mean and the black crosses the max. and min. values. The boxes represents the 25th (lower line), 50th (middle line) and 75th (top line) percentiles. The end of the vertical bars denote the 10th (below the box) and 90th (above the box) percentiles. Stations north and south of the Alps are sorted from the left to the right from the nominal most traffic-influenced station (see Table 1) to the most rural one. Data from the yearly cycle in ZUR are excluded. Only averages ± standard deviations are displayed for stations from which only filters from one winter were analyzed. The Whisker box plots showing the absolute concentrations are presented in Fig. S3 in the Supplementary Material.

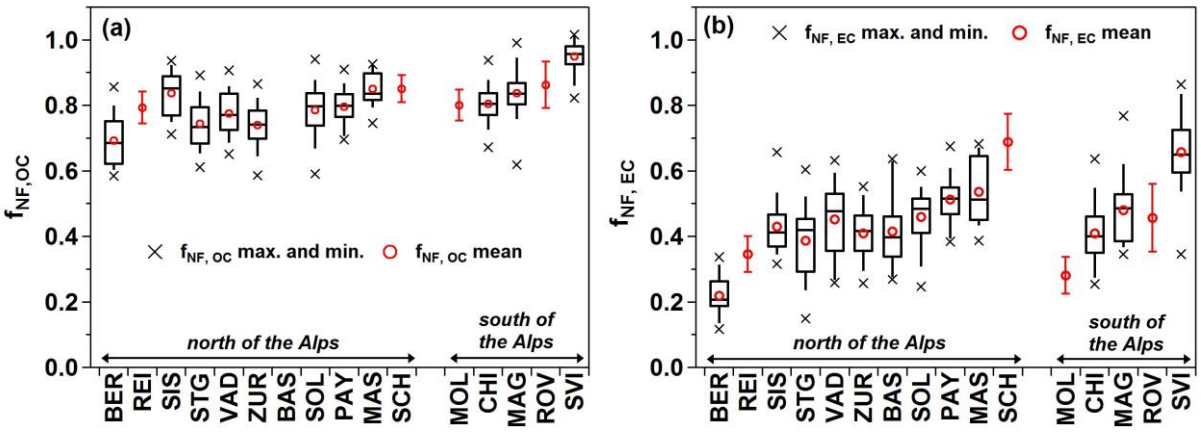

Figure 3: Whisker box plots of the fractional non-fossil contributions of OC (a) and EC (b) summarizing all winter filter samples measured for ^{14}C (n ~ 300 for OC and EC). Stations north and south of the Alps are sorted from the left to the right from the nominal most traffic-influenced station (see Table 1) to the most rural one Only averages ± standard deviations are displayed for stations from which only filters from one winter were analyzed. $f_{NF,OC}$ values for BAS are not included since several values above one were found (see Sect. 3.2). Data from the yearly cycle in ZUR are excluded as well.

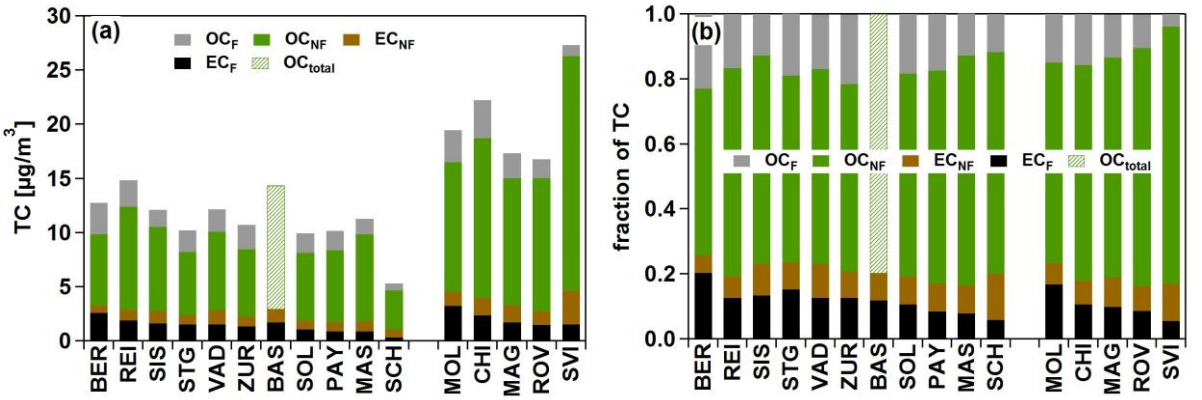

Figure 4: Average over all analyzed winter samples (n ~300) for each station of EC_F, EC_{NF}, OC_{NF} and OC_F (a) as well as their relative contribution to TC (b). Total OC is displayed for BAS since $f_{NF,OC}$ values for this station are not included in the analysis due to several values above one (see Sect. 3.2.1). Data from the yearly cycle in ZUR are excluded as well.

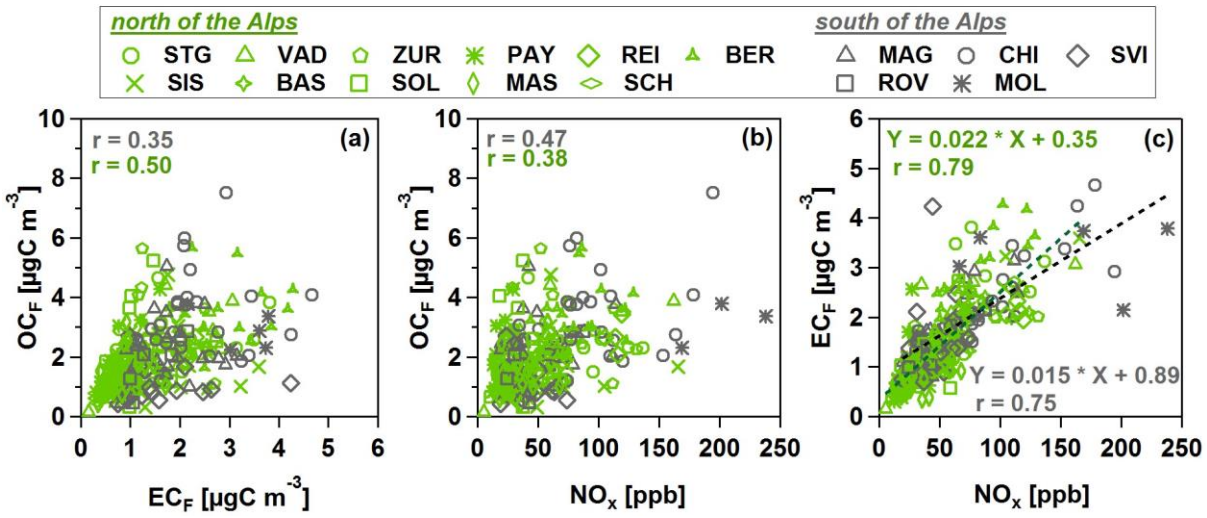

Figure 5: Comparison for stations north and south of the Alps for (a) EC_F and OC_F, (b) NO_x and OC_F as well as (c) NO_x and EC_F. OC_F values from BAS and all data from the yearly cycle in ZUR are excluded (see Sect. 3.2.1 and Sect. 1). An orthogonal distance regression was used to fit the data.

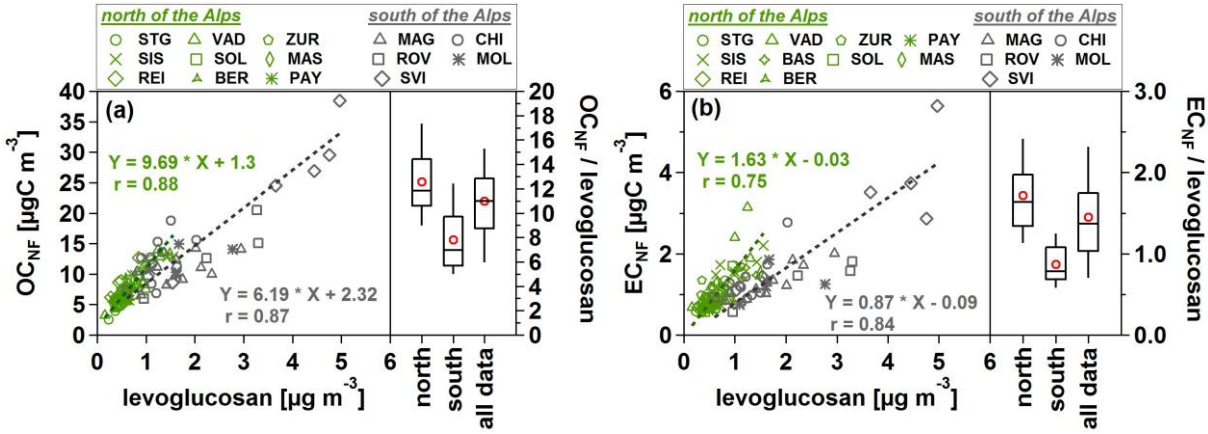

Figure 6: Scatter plot of OC_{NF} (a) and EC_{NF} (b) vs. levoglucosan combined with Whisker box plots of their ratios for all measured winter samples (red circles denote the mean). OC_{NF} values from BAS and all data from the yearly cycle in ZUR are excluded (see Sect. 3.2.1 and Sect. 1). Levoglucosan data is only available for the first two winter seasons (see Table 2). An orthogonal distance regression was used to fit the data.

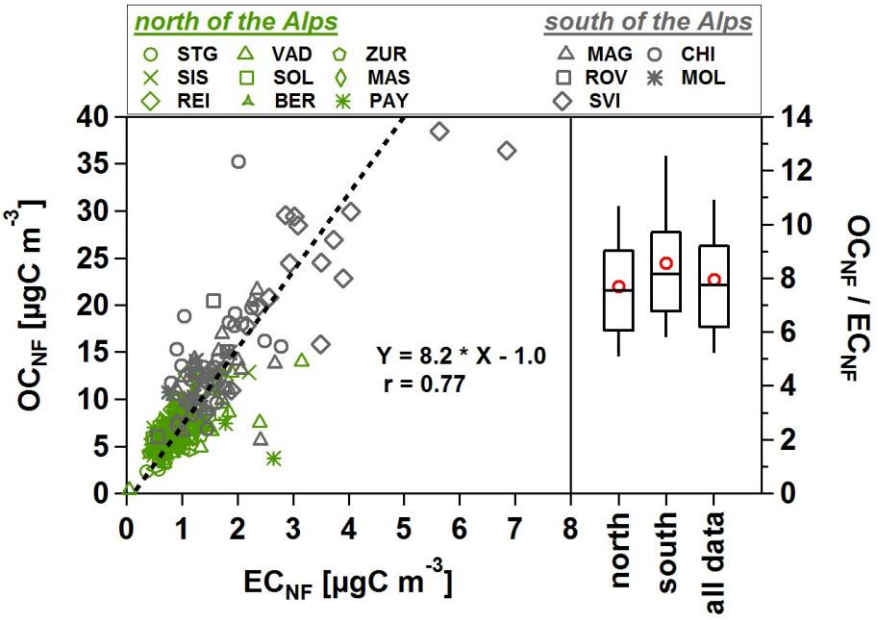

Figure 7: Comparison of OC_{NF} and EC_{NF} combined with Whisker box plots of their ratios for all measured winter samples (red circles denote the mean). OC_{NF} values from BAS and all data from the yearly cycle in ZUR are excluded (see Sect. 3.2.1 and Sect. 1). An orthogonal distance regression was used to fit the data.

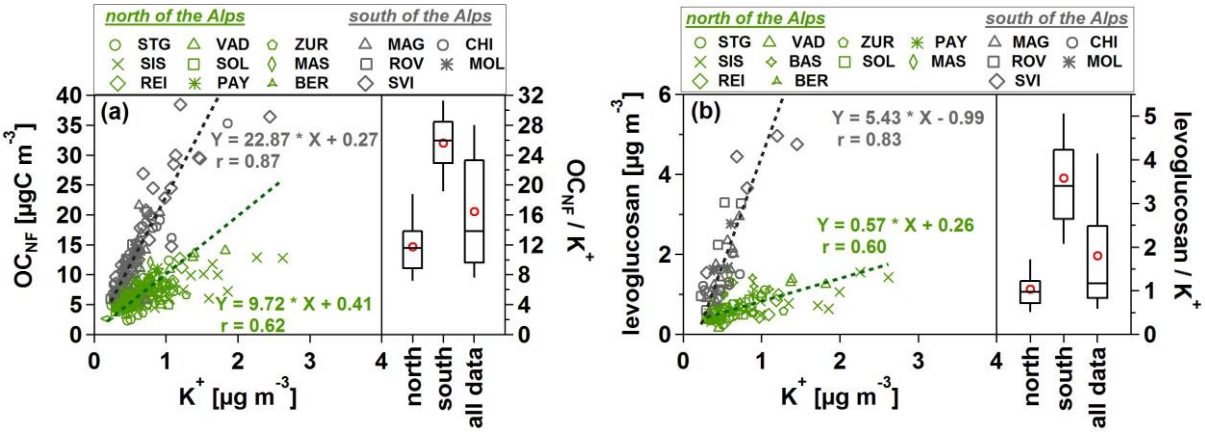

Figure 8: OC_{NF} (a) and levoglucosan (b) as a function of the K^+ concentrations combined with Whisker box plots of their ratios for all measured winter samples (red circles denote the mean). OC_{NF} values from BAS and all data from the yearly cycle in ZUR are excluded (see Sect. 3.2.1 and Sect. 1). Levoglucosan data is only available for the first 2 winter seasons (see Table 2). An orthogonal distance regression was used to fit the data.